

Delivery of chemo-sensitizing siRNAs to HER2⁺-breast cancer cells using RNA aptamers

Kristina W. Thiel¹, Luiza I. Hernandez¹, Justin P. Dassie^{1,2}, William H. Thiel¹,
Xiuying Liu¹, Katie R. Stockdale¹, Alissa M. Rothman¹, Frank J. Hernandez¹,
James O. McNamara II¹ and Paloma H. Giangrande^{1,3,*}

¹Department of Internal Medicine, ²Department of Molecular and Cellular Biology Program and ³Department of Radiation Oncology, University of Iowa, Iowa City, IA 52242, USA

Received June 21, 2011; Revised March 16, 2012; Accepted March 19, 2012

ABSTRACT

Human epidermal growth factor receptor 2 (HER2) expression in breast cancer is associated with an aggressive phenotype and poor prognosis, making it an appealing therapeutic target. Trastuzumab, an HER2 antibody-based inhibitor, is currently the leading targeted treatment for HER2⁺-breast cancers. Unfortunately, many patients inevitably develop resistance to the therapy, highlighting the need for alternative targeted therapeutic options. In this study, we used a novel, cell-based selection approach for isolating 'cell-type specific', 'cell-internalizing RNA ligands (aptamers)' capable of delivering therapeutic small interfering RNAs (siRNAs) to HER2-expressing breast cancer cells. RNA aptamers with the greatest specificity and internalization potential were covalently linked to siRNAs targeting the anti-apoptotic gene, Bcl-2. We demonstrate that, when applied to cells, the HER2 aptamer-Bcl-2 siRNA conjugates selectively internalize into HER2⁺-cells and silence Bcl-2 gene expression. Importantly, Bcl-2 silencing sensitizes these cells to chemotherapy (cisplatin) suggesting a potential new therapeutic approach for treating breast cancers with HER2⁺-status. In summary, we describe a novel cell-based selection methodology that enables the identification of cell-internalizing RNA aptamers for targeting therapeutic siRNAs to HER2-expressing breast cancer cells. The future refinement of this technology may promote the widespread use of RNA-based reagents for targeted therapeutic applications.

INTRODUCTION

While the overall mortality rate for breast cancer has decreased over the past several years due to an increased emphasis on early detection, mortality rates for women with aggressive tumors are still high (1–4). This is primarily a consequence of the overall disease complexity and the general lack of safe and effective therapies for these malignant tumors. A key player in breast cancer malignancy is the human epidermal growth factor receptor 2 (HER2) (5,6). HER2 belongs to the epidermal growth factor receptor (EGFR) family that includes four major proteins: EGFR (also known as HER1 or ErbB1), HER2 (p185 neu/ErbB2), HER3 (ErbB3) and HER4 (ErbB4) (6–10). HER2⁺-breast cancers tend to be more aggressive and more likely to become resistant to therapy than cancers lacking HER2 expression (7,8). The elevated extracellular membrane expression of HER2 in cancer cells, together with the overexpression in both primary tumors and metastatic sites, makes HER2 an ideal candidate for targeted therapies (11,12). As such, targeted inhibition of HER2 represents one of the most validated therapeutic modalities for treating many human cancers, including ovarian (13), gastric (14,15), bladder (16), salivary (17) and lung carcinoma (18).

Trastuzumab (Herceptin), a humanized, inhibitory, monoclonal antibody (mAb) directed against the extracellular domain of HER2, is the current first line treatment administered to patients with HER2⁺-breast cancers (19,20). Many patients who undergo treatment with Trastuzumab are either insensitive to or eventually develop resistance to the drug, highlighting the need for novel targeted therapies (21–27).

Several mechanisms of resistance or insensitivity to HER2 inhibition by Trastuzumab have been described (28–30). One mechanism involves the upregulation of

*To whom correspondence should be addressed. Tel: +1 319 384 3242; Fax: +1 319 353 5552; Email: paloma-giangrande@uiowa.edu

The authors wish it to be known that, in their opinion, the first three authors should be regarded as joint First Authors.

© The Author(s) 2012. Published by Oxford University Press.

This is an Open Access article distributed under the terms of the Creative Commons Attribution Non-Commercial License (<http://creativecommons.org/licenses/by-nc/3.0>), which permits unrestricted non-commercial use, distribution, and reproduction in any medium, provided the original work is properly cited.

other receptor tyrosine kinases (RTKs) that can compensate for loss of HER2 [e.g. insulin-like growth factor-1 receptor (IGF-1R) (31–33), EGFR (34,35), HER3 (36,37) and EphA2 (38)]. Interestingly, a new HER2 splice variant (HER2 Δ 16) with potent transforming activity has also been implicated in therapeutic resistance (39–43).

Survival of HER2⁺-cancer cells can also depend on elevated expression of anti-apoptotic genes that encode proteins such as Bcl-2 (44–49), Bcl-xL (50), survivin (51–57) and XIAP (56). Importantly, elevated Bcl-2 expression has been shown to inhibit chemo-induced apoptosis in human breast cancer cells (49). Not surprisingly, inhibition of Bcl-2 by small molecule inhibitors or RNA interference (RNAi) induces apoptosis in HER2⁺-breast carcinomas and sensitizes tumor cells to chemotherapeutic drugs. This highlights the potential of Bcl-2 specific inhibitors for the treatment of breast tumors with HER2⁺-status that fail to respond to HER2-inhibition (42,48,58–60).

RNA interference (RNAi) is a highly conserved biological process that mediates post-transcriptional gene silencing (61). Since its discovery, RNAi has been used as a tool to dissect gene function, as well as for therapeutic development of several human pathologies (62,63). Importantly, numerous reports have appeared over the past several years describing the use of RNAi to target genes involved in known oncogenic pathways (64–66). In many of these studies, RNAi has resulted in significant reduction in cancer cell proliferation, enhanced apoptosis or increased sensitivity of refractory cancer cells to chemotherapy/radiation (58,64,65,67–69). However, despite the development of a number of effective anticancer cell small interfering (si)RNAs, there are no approved siRNA-based therapies for the treatment of cancer. The major problem for the successful translation of siRNAs into effective therapies in the clinic is delivery (66,70–73). Two aspects of the delivery problem that need to be addressed are: (i) targeted delivery with respect to cell type and (ii) delivery into the cytoplasm of cells *in vivo*.

Toward this end, we have previously utilized an RNA ligand (aptamer) that binds the prostate cancer surface antigen PSMA to selectively deliver cytotoxic siRNAs to prostate cancer cells (68,74). We demonstrated that upon binding to PSMA on the surface of prostate cancer cells, the aptamer with its siRNA cargo (aptamer-siRNA chimera) undergoes endocytosis. Once inside the cell, the aptamer-siRNA chimera acts as a substrate for the RNAi pathway protein Dicer. This, leads to the silencing of the siRNA target gene and the death of PSMA⁺-prostate cancer cells in culture and *in vivo* (68,74).

While this technology holds great potential for delivering functional siRNAs into cells, one of the requirements for its application to other cell types is the identification of specific cell-surface receptors overexpressed on the cells of interest that can be targeted with RNA aptamers. To bypass this hurdle and select for RNA sequences that are efficiently internalized into cells, we have modified the standard SELEX (systematic evolution of ligands by exponential enrichment) methodology to enable the rapid isolation of aptamers for siRNA delivery that selectively

internalize into target cells (Figure 1A). Rather than a trial-and-error approach to finding receptors that will serve as good targets for aptamer-siRNA cargos, this cell-based selection strategy allows us to directly select for sequences that internalize into a particular cell type. Using the ‘cell-internalization SELEX’ approach, we enriched for RNA sequences that bind to HER2 and selectively internalize into HER2⁺-breast cancer cells. The aptamers with the greatest specificity and internalization potential were conjugated to siRNAs targeting the pro-survival gene Bcl-2. The resulting aptamer-siRNA chimeric RNAs exhibit potent silencing of Bcl-2 expression and sensitize HER2-expressing breast cancer cells to chemotherapy, demonstrating the potential of this approach for the treatment of breast tumors with HER2⁺-status.

MATERIALS AND METHODS

Cell lines

N202.1A and N202.1E cells (75,76) were generously provided by G. Forni (University of Torino, Italy). N202.1A is a mammary carcinoma clonal cell line derived from a mammary tumor from the HER2/*neu* transgenic mouse of FVB background. N202.1A cells express high levels of surface HER-2/*neu*, while the N202.1E clonal cell line has no detectable surface expression of the HER2/*neu* oncoprotein. All cell lines were maintained in NuAire water-jacketed CO₂ incubators at 37°C with 5% CO₂. N202.1A (HER2⁺) and N202.1E (HER2⁻) cells were cultured in Dulbecco’s Modified Eagle Medium (DMEM) supplemented with 20% fetal bovine serum (FBS, HyClone). Murine mammary tumor cell lines 78717 (HER2⁻) and 85819 (HER2⁺) (77,78), were generously provided by A. Thor and B. Liu (University of Colorado Denver School of Medicine) and maintained in culture in a 1:1 mixture of DMEM and Ham’s F12 medium containing 10% FBS. The 78717 (HER2⁻) and 85819 (HER2⁺) cell lines were derived from mammary tumors from wild-type rat *c-neu*/ErbB2 transgenic mice. Over several passages in culture, the 78717 (HER2⁻) cell line retained little-to-no HER2 expression. NMuMG cells, derived from normal mouse mammary epithelial cells (ATCC; cat# CRL-1636), were cultured in DMEM supplemented with 10% FBS, 10 µg/ml insulin and 4.5 g/l glucose. Wild-type and Bcl-2^{-/-} mouse embryonic fibroblasts (MEFs) were provided by S. Oakes (University of California, San Francisco) and cultured in DMEM supplemented with 10% heat-inactivated FBS (79).

Western-blot analysis of cell lysates

For western blotting, confluent 100 mm dishes of cells were placed on ice and washed twice with DPBS. Cells were scraped off the plates and incubated for 30 min in RIPA lysis buffer [1% deoxycholate, 1% Triton X-100, 0.1% SDS, 150 mM NaCl, 1 mM EDTA, 50 mM Tris-HCl, pH 7.4 and protease inhibitor cocktail (Sigma)]. Samples were centrifuged at 4°C to remove the insoluble cell pellets and a protein assay was performed to check

protein quantity. Equal amounts of protein sample were prepared in 4× SDS with Laemmli SDS-sample buffer and boiled for 10 min at 95°C. Proteins were resolved on a 7.5% polyacrylamide gel. The proteins were transferred to a PVDF membrane for 2 h at 200 mA. The PVDF membrane was stained for 1 min with Ponceau Red to verify transfer efficiency. The membrane was initially blocked in 5% milk in DPBS for 1 h at room temperature and then incubated with primary antibodies against either HER2 (Ab-3, Calbiochem, OP15), Bcl-2 (BD Pharmingen, clone 3F11; cat# 554218), Bcl-xL (BD Transduction Laboratories, Cat# 610211), ERK1 K-23 (Santa Cruz Biotechnologies Inc., sc-94) and actin (Sigma cat# A5441) in Block Buffer for 2 h at room temperature. The membrane was washed three times with DPBS-0.05% NP-40 before probing with secondary antibodies conjugated to HRP (Amersham). The membrane was incubated at room temperature for 1 h before it was washed three times again with DPBS-0.05% NP-40. Protein bands were visualized with an enhanced chemiluminescent (ECL) system (GE Healthcare).

Flow cytometry

For cell-surface HER2 staining, cells were cultured in 60-mm dishes and harvested at a density of 1×10^6 cells/ml with 0.25% trypsin. Cells were blocked in Block Buffer (4% FBS in DPBS) for 20 min at room temperature. Cells were then incubated in 100 µl Primary Antibody solution (1:100 dilution of anti-HER2 Ab-4; Calbiochem OP16 in Block Buffer) for 30 min on ice. Cells were washed twice with 500 µl of Block Buffer and incubated in 100 µl of Secondary Antibody solution (1:500 goat α -mouse Alexa Fluor 488 IgG; Invitrogen cat # A11001 in Block Buffer) for 20 min at room temperature. Cell were washed twice with 500 ml of Block Buffer and processed for flow cytometry.

To assess Bcl-2 protein expression, cells were fixed and permeabilized using Cytofix/Cytoperm Buffer (BD Transduction Laboratories) following manufacturer's recommendations. Cells were then incubated in 100 µl of Primary Antibody solution (1:100 dilution of anti-Bcl-2 3F11; BD Pharmingen cat# 554218 in Block Buffer) for 30 min on ice. Cells were washed twice with 500 µl of Block Buffer and incubated in 100 µl of Secondary Antibody solution (anti-hamster IgG-FITC; Santa Cruz Biotechnologies, Inc., SC-2792) for 20 min at room temperature. Cells were washed twice and processed for flow cytometry. All samples were analyzed using FACScan instrument and FlowJo software (Flow Cytometry Core, U Iowa).

Cell-internalization SELEX for HER2 aptamer selection

Cell-internalization SELEX is a modification of the previously described cell-based SELEX (80). First, an RNA library with a 20-nt variable region (5'-GGGAGGACG AU GCGGNNNNNNNNNNNNNNNNNNNNNNNNNNNNCAGA CGACUCGCCCGA-3') was generated by *in vitro* transcription using a mutant Y639F T7 polymerase (81). The *in vitro* transcription reactions for the library and

all subsequent rounds of cell-internalization SELEX were supplemented with 2'-fluoro modified CTP and UTP (TriLink Biotechnologies) to generate RNAs that are nuclease-resistant. All cell incubations were carried out at 37°C with 5% CO₂. In each round of cell-internalization SELEX, RNA aptamer pools (150 nM) supplemented with 100 µg/ml yeast tRNA (Invitrogen) were first incubated on non-target N202.1E (HER2⁻) cells for 30 min to remove aptamers that bind to and are internalized into the non-target cells. Next, the supernatant (containing RNA aptamers that do not internalize into the non-target cells) was transferred to target N202.1A (HER2⁺) cells for 30 min. To increase the stringency of the selection in later rounds of cell-internalization SELEX, internalization time and number of cells were reduced. To remove unbound and surface-bound aptamers, target cells (N202.1A) were washed with ice-cold DPBS adjusted to 0.5 M NaCl (High Salt Wash) for 5 min. Internalized RNA aptamers were then recovered using TRIzol reagent (Invitrogen) following manufacturer's instructions, reverse transcribed into DNA, amplified by PCR (Sel2 5' primer: 5'-TAAT ACGACTCACTATAGGGAGGACGATGCGG-3'; Sel2 3' primer: 5'-TCGGGCGAGTCGT CTG-3') and *in vitro* transcribed to generate an enriched pool of RNA aptamers for the next round of cell-internalization SELEX.

454 sequencing and bioinformatic analyses of aptamer pools

Pools of aptamers from rounds 2, 4, 6, 8 and 9 were sequenced using 454-deep sequencing (U Iowa DNA Sequencing Core Facility). To determine the percent enrichment, the total number of unique sequences in each round was divided by the total number of sequences obtained in each round. Next, all unique sequences were aligned using ClustalX2 (82) and sequences were grouped into families using the output dendrogram as a guide. Sequence families were re-aligned and consensus sequences were determined by calculating the percent distribution of the each nucleotide (A, U, C, G) found at each position. The sequences for individual aptamers used in this study are listed in Supplementary Table S1.

Cell internalization assays

Quantitative Reverse Transcription-PCR (qRT-PCR) method

Target (N202.1A and 85819) and non-target cells (N202.1E, 78717 and NMuMG) were incubated with 100 nM aptamer or aptamer-siRNA chimera for 30 min at 37°C with 5% CO₂. Cells were washed with ice-cold High Salt Wash and RNA was recovered using TRIzol reagent. Samples were normalized to an internal RNA reference control. Specifically, 0.5 pmol per sample M12-23 aptamer (83) was added to each sample along with TRIzol as a reference control. Recovered RNAs were quantitated using iScript One-Step RT-PCR Kit with SYBR Green (Biorad) with a Biorad iCycler. All reactions were done in a 50 µl volume in triplicate with primers specific for RNA aptamers

(Sel2 5' primer: 5'-TAATACGACTCACTATAGGGAG GACGATGC GG-3'; 3' primer: 5'-TCGGGCGA GTCG TCTG-3') and M12-23 reference control (Sel1 5' primer: 5'-GGGGGAATTCTAATACGAC TCACTATAGGGA GAGAGGAAGAGGGGATGGG-3'; 3' primer 5'-GGGG GGATCCAGTACTAT CGACCTCTGGGTTATG-3'). Samples were normalized to M12-23, as well as the PCR amplification efficiency of each aptamer relative to SCR1 control aptamer.

Flow cytometry method

To generate FAM-labeled aptamers, the *in vitro* transcription reaction was supplemented with 3 mM FAM-GTP (TriLink Biotechnologies) as previously described (68). Fluorescently labeled aptamers (1 μ M) were incubated on N202.1A and N202.1E cells for 2 h at 37°C. Cells were washed with ice cold DPBS adjusted to 0.5 M NaCl (High Salt Wash) to remove unbound and surface bound RNAs, trypsinized and internalized aptamers assessed by flow cytometry. Samples were analyzed using FACScan instrument and FlowJo software (Flow Cytometry Core, U Iowa).

Fluorescence microscopy method

N202.1A and N202.1E cells were grown in MatTek 35-mm glass bottom culture dishes in DMEM medium supplemented with 20% FBS (HyC). Cells were seeded at a density of 2×10^5 cells/ml in a volume of 250 ml, 1 day prior to the experiment. Cells were allowed to settle for 4 h before the addition of extra 2 ml of media to each dish. On the day of the experiment, cells were washed with pre-warmed DPBS buffer and incubated for 90 min at 37°C with FAM-labeled aptamers (1 μ M). Next, cells were washed twice with ice cold DPBS adjusted to 0.5 M NaCl (High Salt Wash) to remove unbound and surface bound RNAs. Subsequently, cells were fixed with 3.7% formaldehyde for 20 min at room temperature. DAPI nucleic stain was performed by adding DAPI to 1 g/ml final concentration at room temperature for 10 min followed by washing three times with DPBS. Images of the internalized aptamers were acquired with a 40 \times oil objective of an Olympus IX71 inverted equipped with a CCD camera and filters for FITC (excitation BP450-490, emission BP515-565) and DAPI (excitation D360/40, emission D460/50). The fluorescence images reported here are representative of at least three captured images per dish/per condition. Fluorescence signal is given by the internalized aptamer and intra-cellular localization is confirmed by overlaying the fluorescence images with the nuclear DAPI stain and subsequently, with the phase/contrast images using ImageJ 1.46 d software.

SPR measurements

All measurements were performed with a Biacore 3000 in Binding Buffer (200 mM HEPES pH 7.4, 100 mM NaCl, 20 mM CaCl₂, 0.1% BSA). The immobilization of HER2 aptamers (E1, C1 and B1) on streptavidin chips (SA) was performed under standard conditions recommended by the manufacturer (GE BIAcore) and protocols previously described (84,85) HER2 aptamers were previously biotinylated at 3'-end by transcription (83). The flow

rate was set at 5 μ l/min and the biotinylated HER2 aptamers were injected at a concentration of 1 μ M over the SA sensor chip for 10 min at 25°C. The unbound aptamers were removed by treatment with 50 mM aqueous NaOH and the chip was primed before use. Recombinant rat HER2 protein (rHER2) (GenWay, cat#1028823186) was injected over the sensor surface for 5 min (association and dissociation time). Four concentrations of rHER2 protein were injected by serially diluting samples from 40 to 5 nM. The selectivity studies were carried out by injecting 40 nM of each, BSA, hHER2 and hEphA2 protein (R&D Systems, cat#3035A2) over HER2 immobilized aptamers. The injections for these control samples were performed under the same conditions described earlier. After each run, the surface was regenerated with 50 mM aqueous NaOH for 5 s at 15 μ l/min. The raw data was processed and analyzed to determine the binding constant for HER2 aptamers. To correct for refractive index changes and instrument noise, the response of the control surface data was subtracted from the responses obtained from the reaction surface using BIA evaluation 4.1. The K_D for each aptamer was calculated by global fitting of four concentrations of rHER2 protein, assuming a constant density of HER2 aptamers on the surface of the chip. A 1:1 binding mode with mass transfer fitting was used to obtain the kinetic data. BSA, hHER2 and hEphA2 measurements were aligned to rHER2 data for the non-specific analysis

Silencing of Bcl-2

Bcl-2 siRNA [target sequence: 5'-AAGCTGTACAGAG GGGCTAC-3'; (79)] or control non-silencing siRNA (Accell D001910-01, Dharmacon) were transfected using Oligofectamine (Invitrogen) according to the manufacturer's instructions. To assess silencing at the mRNA level, total RNA was recovered using RNeasy kit (Qiagen) and murine Bcl-2 expression was determined by qRT-PCR (5' primer: 5'-GAACTATATGGCCCCAGC AT; 3' primer: 5'-CAGGTATGCACCCAGAGTGA). Samples were normalized to murine GAPDH mRNA expression (5' primer: 5'-ACCCAGAAGACTGTGGAT GG-3'; 3' primer, 5'-CACATTGGGGGTAGGAAC AC-3'). To assess silencing at the protein level, Bcl-2 or control siRNAs were transfected as described earlier and 48-h post-transfection cells were lysed with RIPA buffer. Equal volumes of each lysate were separated by SDS-PAGE and blotted with an antibody to Bcl-2 (BD Pharmingen, clone 3F11; cat# 554218).

Chimera generation

Double-stranded DNA duplexes for transcription were generated by PCR as described in McNamara *et al.* (68) and Dassie *et al.* (74). Briefly, primers and templates for generating the individual duplexes are listed: DNA templates for the HER2 aptamers are listed in Supplementary Table S1. Sel2 primer 5'-TAATACGACTCACTATAGG GAGGACGATGCGG-3'; Bcl-2 primer: 5'-AAGTAGC CCCTCTGTGACAGCTCGGGCGAGTCGTCTG-3'. PCR-amplified DNA duplexes were purified with Qiagen DNA purification columns and used for *in vitro*

transcription reactions as described in McNamara *et al.* (68). The longer strands of the HER2 aptamer-Bcl-2 siRNA chimeras were engineered by adding nucleotides complementary to the Bcl-2 antisense sequence to the 3' termini of the HER2 RNA aptamers. All RNAs generated by *in vitro* transcription were produced with 2'fluoro modified pyrimidines to render the RNAs resistant to nuclease degradation. Sequences of the respective long RNA strands are listed in Supplementary Table S2. A 4-fold molar excess of the Bcl-2 antisense sequence (79) was annealed to each long RNA strand (at a final concentration of 1 μ M) by heating the long RNA strand at 95°C for 10 min, adding the 4-fold excess antisense siRNA strand to the unfolded aptamer solution and transferring the mixture to a 65°C dry bath for 7 min. The RNA mixture was allowed to cool at 25°C for 20 min to allow annealing of the two RNA strands. RNA aptamers and siRNAs were folded and annealed in 1XBB (20 mM HEPES pH 7.4, 150 mM NaCl, 2 mM CaCl₂) as previously described (68,74). The excess antisense siRNA strand was removed by filtering the folded RNAs through Amicon Y-30 columns (Millipore, UFC803024).

5'-rapid amplification of cDNA ends (5'-RACE) PCR analysis

mRNA (10 ng) from N202.1A cells treated with different chimeras was ligated to a GeneRacer adaptor (cat #: L1502-01; Invitrogen, Carlsbad, CA, USA) without prior treatment. Ligated RNA was reverse transcribed using a gene-specific primer (GSP1_mBcl2: 5'-GGGTCA GATGG ACCACAGGT-3'). In order to detect cleavage products, PCR was performed using primers complementary to the RNA adaptor (GR5'pr: 5'-CGACTGGAGCA CGAGGACACTGA-3') and gene-specific primer 2 [Gene Specific Primer 2: (mBcl2-v1/2-3'pr): 5'-CAGGCTGGAA GGAG AAGATG-3']. The amplification products were resolved by agarose gel electrophoresis and visualized by ethidium bromide staining. The identity of the specific PCR products was confirmed by sequencing of the excised bands.

Cell death and apoptosis

IC₅₀ measurements

N202.1E (HER2⁻) and N202.1A (HER2⁺) cells were incubated with increasing amounts of cisplatin (ranging from 0 to 100 μ M) for 24 h. Cell viability was measured using the MTS [3-(4,5-dimethylthiazol-2-yl)-5-(3-carboxymethoxyphenyl)-2-(4-sulfophenyl)-2H-tetrazolium] assay according to manufacturer's protocol (Promega Part# TB245: CellTiter96 Aqueous One Solution Cell Proliferation Assay).

Chimeras

N202.1A (HER2⁺) cells were incubated with either HER2 aptamer-Bcl-2 siRNA or HER2 aptamer-Con siRNA chimeras (200 nM) for 72 h then low-dose cisplatin (20 μ M) was added for an additional 24 h. Apoptosis was assessed using an antibody against activated caspase-3 (BD Pharmingen, cat# 550914) following the manufacturer's protocol. As a positive control for

apoptosis, cells were incubated with high dose cisplatin (80 μ M). Scrambled RNA chimeras (Scr1-Bcl-2 and Scr2-Bcl-2), with the aptamer sequences scrambled to abrogate binding to HER2, were used as negative controls for this experiment.

RESULTS

Identification of RNA aptamer sequences that selectively internalize into rat HER2-expressing cells

Aptamers that selectively internalize into rat HER2 expressing mouse mammary carcinoma cells (N202.1A) were isolated using the 'cell-internalization SELEX' protocol (Figure 1A). The advantage of the 'cell-internalization SELEX' over conventional SELEX methodologies is that it enriches for sequences that: (i) bind to the target receptor in the context of the cell membrane and (ii) internalize into the target cells.

Target N202.1A(HER2⁺) cells were derived from an established ratHER2/*neu* transgenic mouse model of mammary carcinoma (75,76). To enable the identification of target-specific sequences, a counter-selection step against matched control cells that do not express rat HER2 (N202.1E) was introduced. HER2 expression in N202.1A cells was verified using immunoblotting (Figure 1B, left panel) and flow cytometric analysis (Figure 1B, right panel) with antibodies specific to rat HER2. Importantly, to enrich for RNA sequences that internalize into the target cells, we introduced a stringent salt wash to remove any unbound RNA and to reduce surface-bound RNAs (Supplementary Figure S1). Nine rounds of selection (against target N202.1A cells) and counter-selection (against N202.1E cells) were performed. Cell-specific internalization of the RNA pools at each round of selection was verified using quantitative PCR (Figure 1C). High throughput, 454 sequencing and bioinformatics analysis of thousands of selected RNA sequences from rounds 2, 4, 6, 8 and 9 of the selection revealed that the selection converged between rounds 6 and 8 (Figure 1D). Rapid convergence is likely a result of the short RNA sequence library (51-mer) used for the selection (86). The percent enrichment at each round of selection was measured by taking the total number of unique sequences in each round and dividing by the total number of sequences obtained in each round as previously described (86).

Sequences were aligned into families based on their primary sequence homology (Figure 2A). This analysis revealed five major sequence families (Family A–E). Consensus sequences were determined by calculating the percent distribution of each nucleotide (A, U, C, G) found at a given position (Figure 2A, left panel). The percent enrichment was measured to determine the evolution of each sequence family at the later rounds of selection (rounds 6, 8 and 9) (Figure 2A, right panel). The sequences for individual RNA aptamers identified in this study are listed in Supplementary Table S1. Theoretical secondary structures, based on the consensus sequences for each family, were generated using RNAstructure algorithm (Figure 2B). Interchangeable nucleotides in the

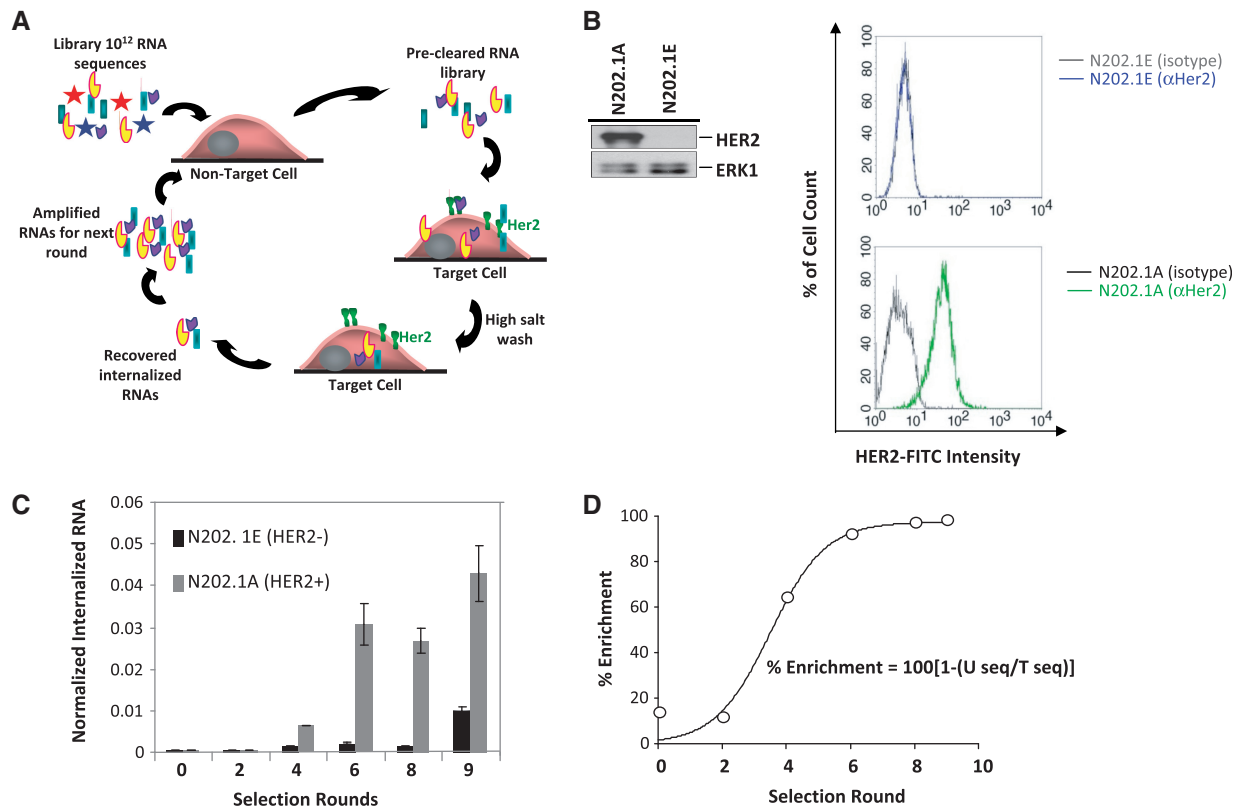


Figure 1. Cell-Internalization SELEX (systematic evolution of ligands by exponential enrichment). (A) Schematic of the methodology used to isolate aptamers that specifically internalize into HER2-expressing cells. (B) Equal amount of lysates from N202.1A(HER2⁺) and N202.1E(HER2⁻) mouse mammary carcinoma cells were blotted for HER2 protein (*left panel*). ERK1 was used as a loading control for total protein. Cell surface expression of HER2 on N202.1A(HER2⁺) cells was confirmed by flow cytometry using non-permeabilized cells stained with either isotype control antibody (gray) or HER2 antibody conjugated to FITC (blue: N202.1E; green: N202.1A) (*right panel*). (C) Nine rounds of cell-internalization SELEX were performed to enrich for RNA aptamers that internalize into N202.1A(HER2⁺) cells (target cells). Non-specific aptamers were removed by pre-clearing against N202.1E(HER2⁻) cells (non-target cells). Progression of the selection was monitored using quantitative RT-PCR (qRT-PCR) and normalizing to an internal RNA reference control for the PCR. (D) Aptamer pools from rounds 0, 2, 4, 6, 8 and 9 were sequenced by 454 sequencing. Enrichment at each round was determined by the indicated formula (U = unique; T = total).

consensus sequences for Families A, C and E are highlighted in red. The overall theoretical secondary structures are conserved with respect to these nucleotides. In the case of Family B, the consensus sequence generated three distinct predicted secondary structures.

Next, we evaluated the internalization potential of several of the single RNA aptamers isolated from the cell-internalization selection process (Figure 2C and D). Individual RNAs were incubated with mouse mammary carcinoma N202.1E(HER2⁻) or N202.1A(HER2⁺) cells. The RNAs that internalized into the cells were recovered by TRIzol extraction and quantified using qRT-PCR (Figure 2C). Importantly, the individual aptamers tested internalized preferentially into HER2 expressing cells (gray bars) compared to the matched control, N202.1E cells lacking HER2 expression (black bars) (Figure 2C). Two scrambled RNA aptamer sequences (Scr1 and Scr2) and the initial, unselected RNA library (R0) were used as negative controls for cell-internalization in this assay. In addition, to verify that the individual RNA aptamers were selectively internalizing into mouse mammary carcinoma cells expressing HER2, we repeated the internalization assay using mammary carcinoma cells derived from an

analogous rat HER2 transgenic mouse model (77,78) (Figure 2D). As predicted, the RNA aptamers internalized specifically into 85819 (HER2⁺) cells (gray bars) and little-to-no internalization was observed in the 78717 cells lacking HER2 expression (Figure 2D). Cell-internalization by the RNA aptamers was specific to cancer cells overexpressing the HER2 receptor. No significant internalization was observed in normal murine mammary epithelial cells (NMuMG) with negligible levels of HER2 protein expression (Supplementary Figure S2). Importantly, this highlights the potential safety of this approach for targeting cancer cells while sparing normal cells.

To rule out any artifacts as a result of the qRT-PCR assay, we verified cell-internalization of selective RNA sequences (A2, B1, C1, D1, E1) from each sequence family using 5'-end FAM-labeled RNA aptamers and flow cytometry (Figure 2E). In these experiments, FAM-labeled RNA aptamers were incubated on live cells. Unbound and surface bound RNAs were removed using the stringent salt wash described earlier (Figure 2C and Supplementary Figure S1). As anticipated, the individual RNAs internalized specifically into N202.1A(HER2⁺)

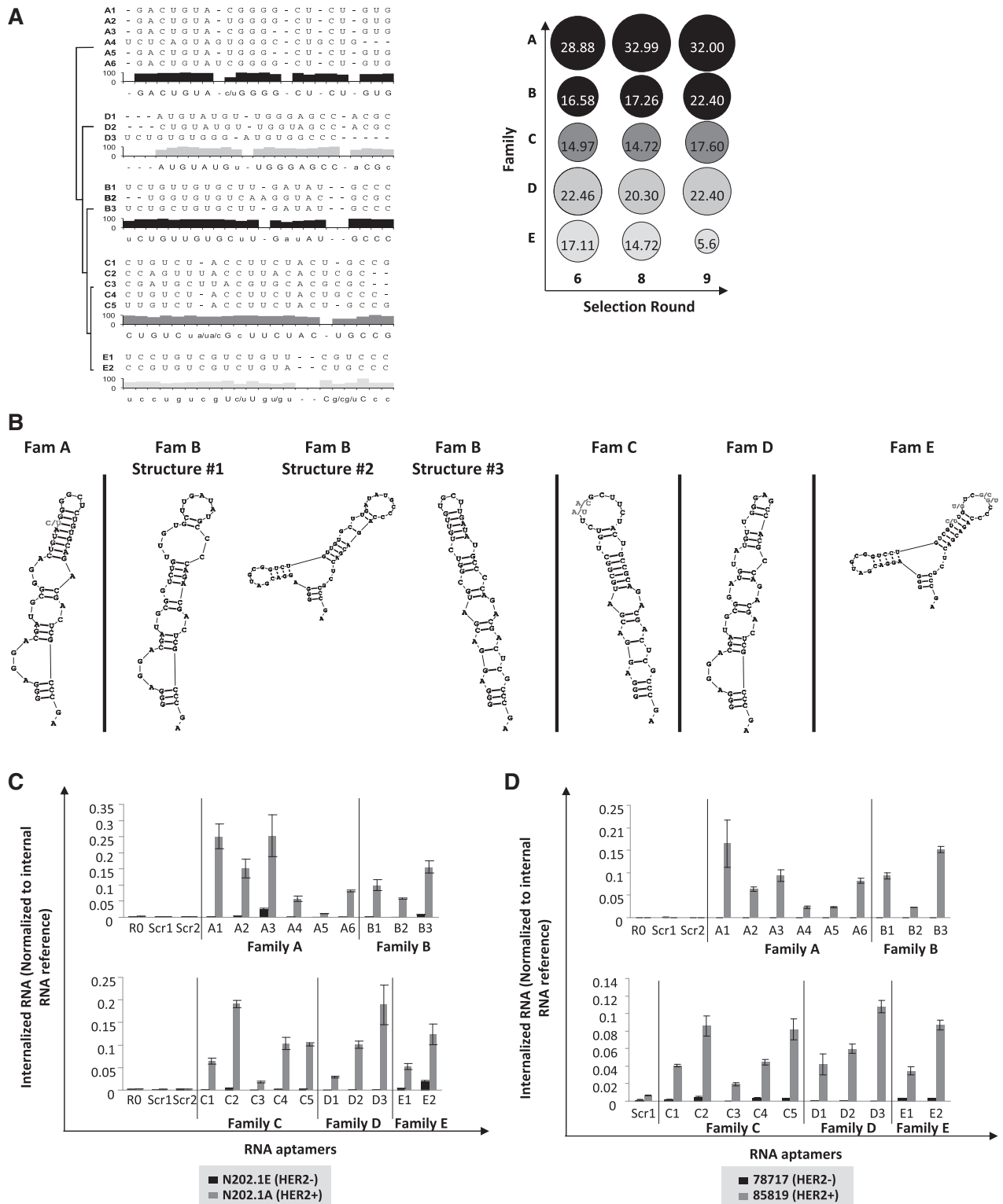


Figure 2. Internalization of single aptamers into HER2⁺-cells. (A) Dendrogram of sequence families with representative RNA aptamers and consensus sequence within each family. The consensus sequence of each family was determined and plotted using the distribution of nucleotides at each position (upper case >75%, lower case <75%, lower case/lower case <50%, gap 0%). The distribution (% of total) of sequence families within each round is shown on the right (circles). (B) Consensus sequences for each family were used to generate predicted secondary structures using RNAstructure algorithm. Interchangeable nucleotides in the consensus sequences for families A, C and E are highlighted in red. These nucleotides do not change the overall predicted secondary structure. The consensus sequence for family B generated three distinct predicted secondary structures. Single aptamers were evaluated for internalization into N202.1E(HER2⁻) and N202.1A(HER2⁺) cells (C) and 78717(HER2⁻) and 85819(HER2⁺) mammary carcinoma cells (D) using qRT-PCR as in Figure 1C. (E) Internalization of fluorescently labeled RNA aptamers into N202.1E(HER2⁻) and N202.1A(HER2⁺) cells was measured by flow cytometry. (F) Confirmation of internalization of fluorescently labeled RNA aptamers (E1 and C1) into N202.1A(HER2⁺) cells using microscopy. A scrambled, non-internalizing aptamer (Scr) was used as a negative control in these experiments. Fluorescence images were overlaid with DAPI and P/C (phase contrast) channels. Arrows indicate perinuclear localization of RNA aptamers.

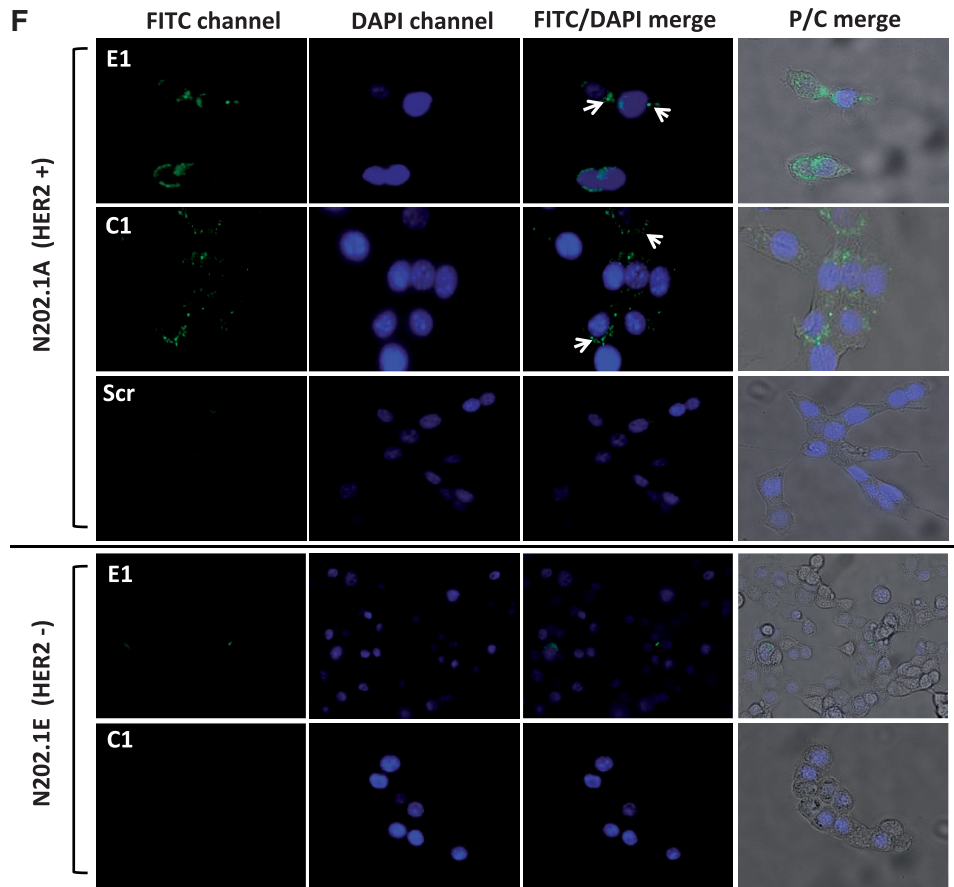
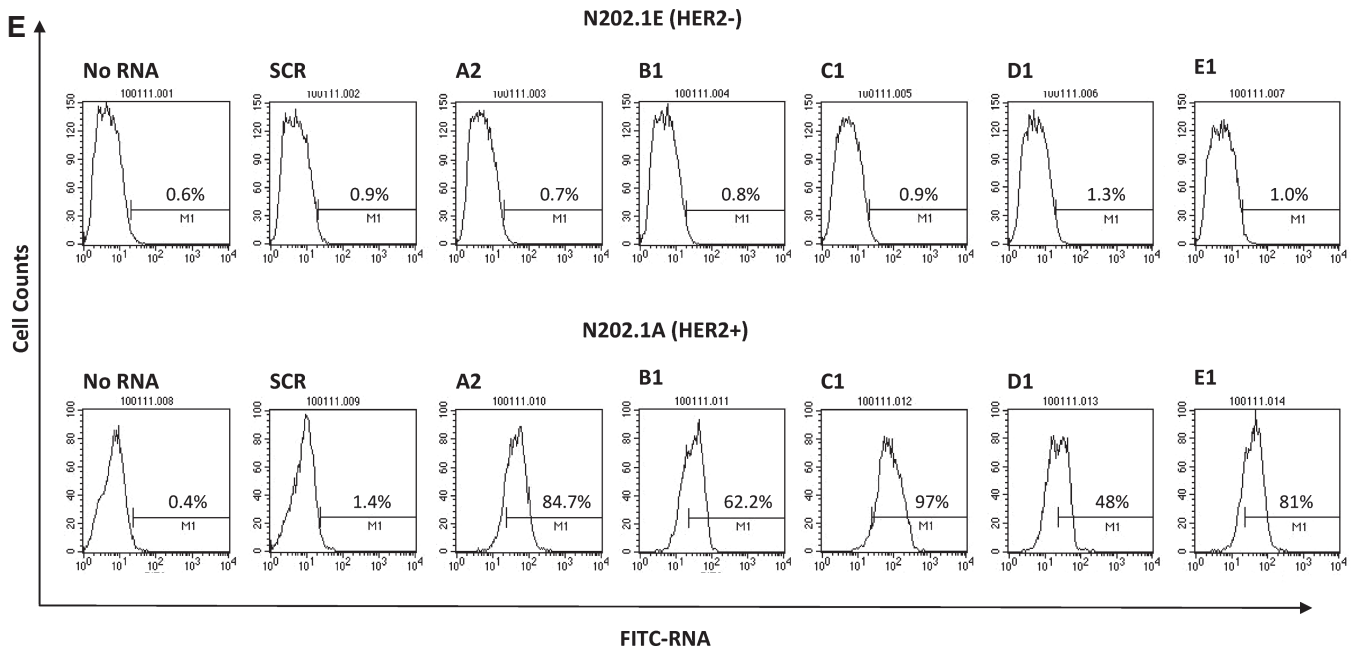


Figure 2. Continued.

cells but not into N202.1E(HER2⁻) cells (Figure 2E). A FAM-labeled, scramble RNA aptamer sequence (Scr) was used as a negative control in this assay and did not internalize.

To rule out the possibility that the RNA aptamers are remaining on the cell surface following the stringent salt wash step, we performed fluorescence microscopy (Figure 2F). In this assay, chemically synthesized C1 and E1 RNA aptamers were conjugated to FAM and incubated with either HER2⁺- (N202.1A) or HER2⁻- (N202.1E) cells for 1 h prior to imaging. Cells were washed with the stringent salt wash and remaining RNAs visualized by fluorescence microscopy. As shown in Figure 2F, aptamers C1 and E1 internalize specifically into HER2⁺-cells but not HER2⁻-cells. We observe perinuclear and cytoplasmic punctuated fluorescence. Furthermore, a negative control RNA aptamer (SCR) does not internalize under these conditions. These data are in support of the Bcl2 silencing data (Figure 5D and E) and confirm that the selected RNA aptamers internalize into HER2-expressing cells.

To address whether the RNA aptamers identified by the cell-based cell-internalization SELEX approach bound directly to HER2, we performed surface plasmon resonance (SPR, BIAcore) on selective RNA aptamers (B1, C1 and E1) using recombinant purified rat HER2 protein (Figure 3). Importantly, all three RNA sequences analyzed, bound with low nanomolar affinity (Figure 3A) and specificity (Figure 3B) to the purified recombinant rat HER2 protein. The respective affinities of the RNA aptamers for purified, recombinant rat HER2 protein are as follows: C1 ($K_D = 45.8$ nM) > E1 ($K_D = 60.8$ nM) > B1 ($K_D = 85.2$ nM) (Figure 3A). Interestingly, the binding affinities of B1, C1 and D1 correlate with the degree of aptamer cell-internalization as observed by flow cytometry (Figure 2E, bottom panel). Binding specificity was demonstrated by examining the binding of B1, C1 and D1 aptamers to analogous receptor tyrosine kinases (RTKs) (e.g. human HER2 and human EphA2) (Figure 3B). All three RNAs tested bound solely to the rat isoform of HER2 and not to the human isoform of the receptor (indicating specificity for the rat isoform) or to a different RTK (human EphA2) (Figure 3B). In addition, for aptamers C1 and E1, specificity for the rat HER2 isoform was confirmed using N202.1A cells expressing human HER2 (data not shown).

Bcl-2 gene expression is elevated in HER2-expressing breast cancer cells

It has been previously documented that Bcl-2 gene expression is elevated in breast cancers (44–49). Moreover, the overexpression of HER2 has been associated with increased Bcl-2 mRNA and protein expression (42,50,60). Herein, we evaluated the expression of the anti-apoptotic gene Bcl-2 in several mouse mammary carcinoma cell lines, both at the mRNA level (Figure 4A, left panel) and at the protein level (Figure 4A, right panel and Supplementary Figure S3A). The relative levels of Bcl-2 mRNA were found to be 2-fold higher in mammary carcinoma cell lines with HER2⁺-status (N202.1A, 85819)

compared to their matched controls (N202.1E, 78717) (Figure 4A, left panel). Bcl-2 wild-type (Bcl-2^{+/+}) and null (Bcl-2^{-/-}) mouse embryo fibroblasts (MEFs) were used as controls for Bcl-2 mRNA levels in these assays. Bcl-2 protein expression in these cell lines was confirmed by immunoblotting (Figure 4A, right panel) and flow cytometric analysis (Supplementary Figure S3B).

To determine the effects of Bcl-2 inhibition in the HER2⁺-mouse mammary carcinoma cells, we identified a small interfering RNA (siRNA) directed against mouse Bcl-2. Silencing was verified in N202.1A cells upon transfection with a cationic agent (Figure 4B). A non-silencing siRNA (Con siRNA) was used as a control for specificity in these assays.

Since elevated Bcl-2 expression has been shown to result in chemotherapeutic resistance in many human cancer cell lines (87–89), we sought to determine the effect of elevated Bcl-2 expression levels in the N202.1A(HER2⁺). As predicted, we demonstrated that elevated Bcl-2 expression renders N202.1A(HER2⁺) cells more resistant to cisplatin treatment (Figure 4C) (N202.1A IC₅₀: 23.2 μM versus N202.1E IC₅₀: 10 μM). Importantly, we demonstrated that silencing of Bcl-2 in N202.1A cells sensitizes the cells to cisplatin treatment, leading to increased apoptosis at low doses of cisplatin (20 μM) (Figure 4D). N202.1A cells were treated with a high dose of cisplatin (80 μM) to achieve comparable cell death (high cisplatin: 67% apoptosis versus combination of Bcl-2 siRNA with low cisplatin: 73% apoptosis). Apoptosis was measured by flow cytometry using an antibody against active, cleaved caspase 3 (Figure 4D).

HER2 aptamer-Bcl-2 siRNA chimeras for targeted delivery of Bcl-2 siRNAs into HER2-expressing cells

We have previously delivered cytotoxic siRNAs specifically to prostate cancer cells using RNA aptamers to prostate cancer-specific membrane antigen (PSMA) (68). In this study, we employed a similar approach for cell-specific targeting of Bcl-2 siRNAs into mouse mammary carcinoma cells expressing rat HER2 with HER2-specific RNA aptamers. The aptamer portion of the chimera, that mediates binding to HER2, was covalently linked to the Bcl-2 siRNA passenger strand (sense strand). The sequences of the aptamer-siRNA sense strands for all chimeras are listed in Supplementary Table S2. The Bcl-2 siRNA guide strand was subsequently annealed to the passenger strand as previously described (68,74). The predicted structures of the HER2 aptamer-Bcl2 siRNA chimeras are shown in Figure 5A, with the Bcl-2 siRNA guide strand sequence highlighted in red. A total of 12 different chimeras were designed corresponding to selective cell-internalizing aptamers from sequence families A through E (Figure 2B and Supplementary Table S1).

To assess whether appending the Bcl-2 siRNA sequence onto the aptamers affected the ability of the aptamers to internalize into N202.1A cells, we performed the cell internalization assay with both HER2 aptamers and chimeras as described earlier (Figure 5B). While appending the siRNA sequence onto the aptamers seemed to

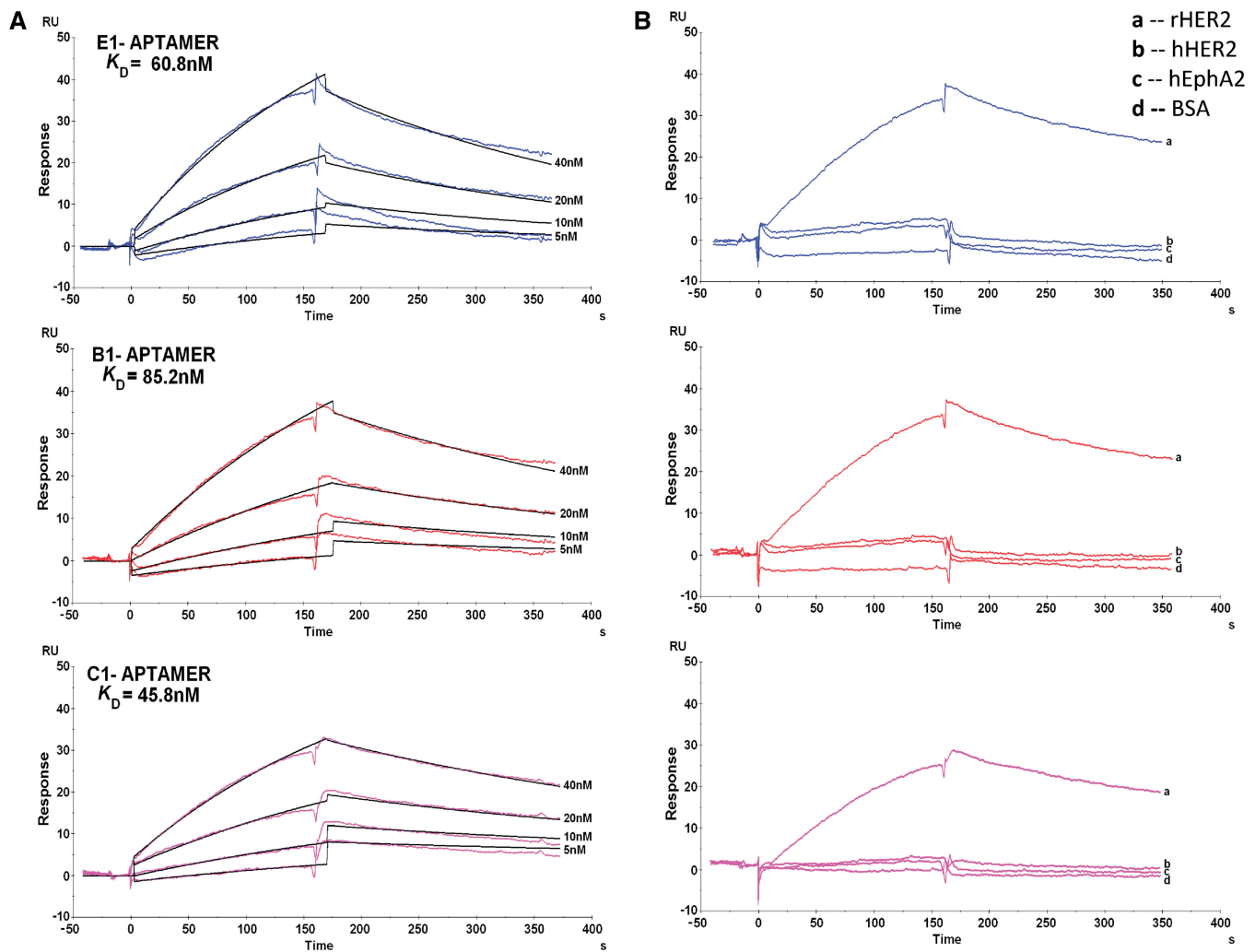


Figure 3. Affinity and specificity analysis of aptamer binding to recombinant HER2 using Surface Plasmon Resonance (SPR). (A) High-affinity interaction between immobilized aptamers (E1, B1 and C1) and rHer2 recombinant protein. Four different rHer2 protein concentrations were analyzed (5–40 nM) and the K_D was reported for each aptamer. The aptamer binding profiles were fitted using Langmuir fitting model (with mass transfer), as determined by BIA evaluation 4.1 software, black lines. (B) Evaluation of the rHer2 protein specificity using three non-specific targets at 40 nM concentration each (b-hHer2; c-hEphA2 and d-BSA), over the immobilized aptamers.

reduce cell-internalization (compare aptamers to chimeras), the chimeras were still internalized specifically in rat HER2 expressing cells N202.1A (Figure 5B) and 85819 (Supplementary Figure S4). However, they were not internalized into N202.1E (Figure 5B) and 78717 cells lacking HER2 expression (Supplementary Figure S4) or normal mammary epithelial cells (NMuMGs) with negligible HER2 surface expression (Figure 5C). Control chimeras composed of the Bcl-2 siRNA appended to two independent scrambled aptamer sequences (SCR1-Bcl-2; SCR2-Bcl-2) were used as negative controls in these assays. No cell internalization was observed in N202.1A, N202.1E or NMuMG cells with the control chimeras. All chimeras were found to internalize, albeit to different degrees, into HER2-expressing breast cancer cells (Figure 5B and C).

To address whether the internalized chimeras were processed by the RNAi machinery and silenced Bcl-2

gene expression, we measured Bcl-2 mRNA levels in N202.1A cells following treatment with the chimeras (Figure 5D, gray bars). Specifically, N202.1A cells were treated with the aptamer-siRNA chimeras or control chimeras (Scr1 and Scr2) in the absence of transfection reagent, for either 38 h (Figure 5D, top panel) or 96 h (Figure 5D, bottom panel). Silencing of Bcl-2 was assessed by the degree of Bcl-2 mRNA knockdown using qRT-PCR (Figure 5D). As controls, cells were treated with non-silencing (C) or Bcl-2 (B) siRNAs alone (negative control, black bars) or transfected into cells (empty bars, positive control). The results show that after 96 h in culture, the degree of Bcl-2 gene silencing achieved with the chimeras (in the absence of transfection reagent) was equivalent to that observed by transfecting (using a cationic lipid) the Bcl-2 siRNA. Together, these data suggest that aptamer-Bcl-2 chimeras are being efficiently delivered to target

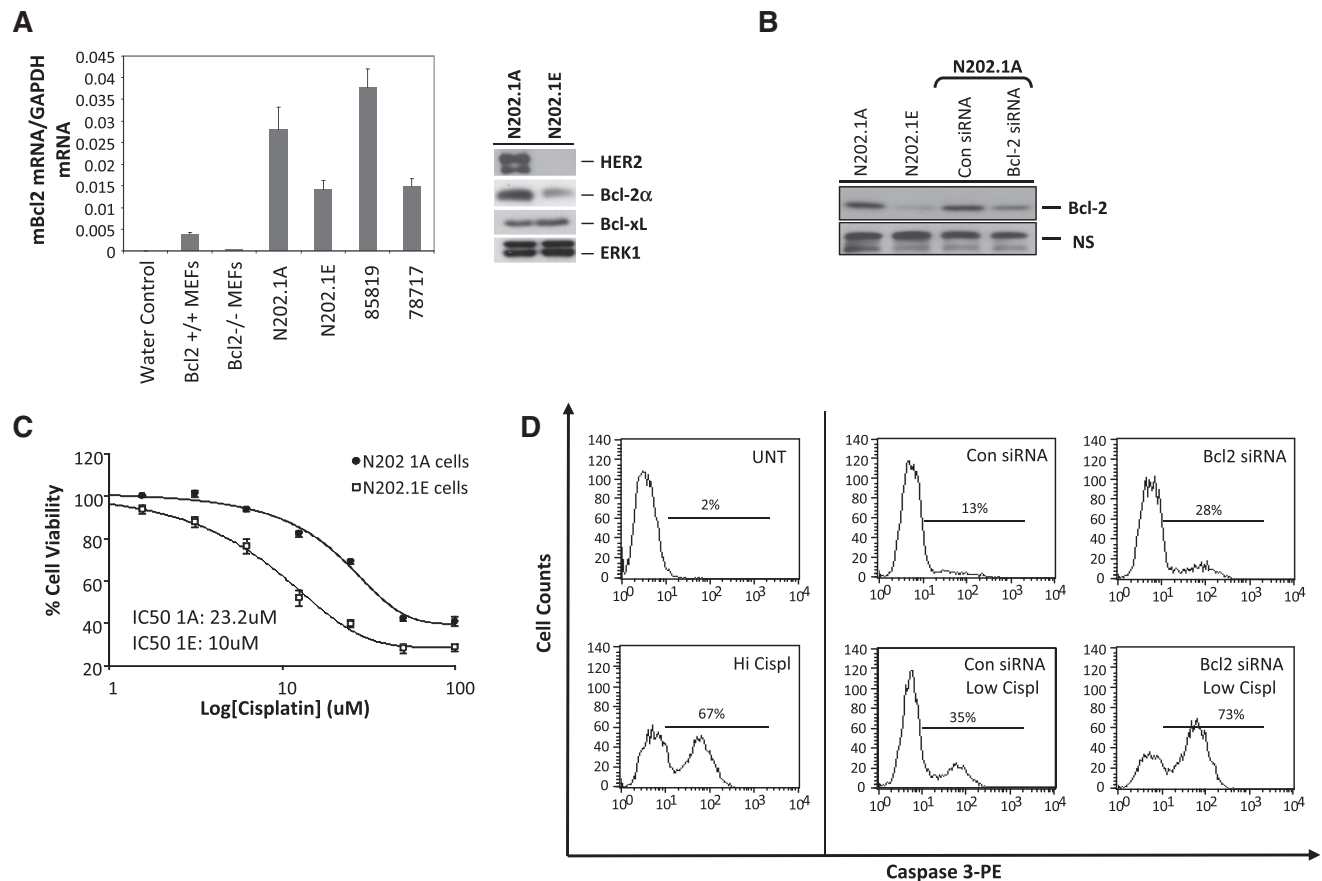


Figure 4. Characterization of Bcl-2 expression in HER2⁺ breast cancer cells. (A) Bcl-2 overexpression at the mRNA level (left panel) was measured in HER2⁺ (wild-type MEFs, N202.1A, 85819) relative to HER2⁻ (Bcl-2^{-/-} MEFs, N202.1E, 78717) cells using qRT-PCR. Values for Bcl-2 mRNA were normalized to GAPDH mRNA for each sample. Bcl-2 protein expression levels (right panel), as assessed by immunoblot analysis, were elevated in N202.1A(HER2⁺) compared to N202.1E(HER2⁻) cells. The protein expression levels of the related family member Bcl-xL were unchanged in the two cell types. The ERK expression level was used as the control of equal protein loading. (B) Western-blot analysis of Bcl-2 protein in N202.1A cells treated with Bcl-2-siRNAs or control non-targeting siRNAs after the liposome-mediated transfection. (C) Viability of N202.1A and N202.1E cells in the presence of increasing amounts of cisplatin. (D) Bcl-2 siRNA sensitizes N202.1A(HER2⁺) cells to cisplatin, resulting in apoptosis (as measured by activation of active cleaved caspase 3) at low cisplatin concentrations (20 μ M). The percent of apoptotic cells was determined by flow cytometry analysis of caspase-3-PE stained cells. High dose cisplatin (80 μ M).

cells, via the HER2 receptor expressed on the surface membrane.

To confirm that the silencing effect by the HER2 chimeras is really due to RNA interference delivered by the chimeric RNAs, we performed 5'-RACE PCR and sequencing data for several of the HER2-Bcl2 chimeras (A1-Bcl2, B1-Bcl2, C3-Bcl2, D1-Bcl2 and E1-Bcl2) (Figure 5E). The mRNA from N202.1A cells previously treated with the above HER2-Bcl2 chimeras was ligated to an RNA adaptor and reverse transcribed using a mouse Bcl2 gene-specific primer. Gel electrophoresis and sequencing of the 5'-RACE PCR products generated with a primer specific to the RNA adaptor and a reverse primer specific to the mouse Bcl2 gene show that Ago2-mediated cleavage occurs between bases 10 and 11 relative to the 5'-end of the guide Bcl2 siRNA strand. PCR products were not observed in samples from control treated cells or cells treated with a non-targeting chimera (SCR-Bcl2) (Figure 5E). These data confirm that the

HER2-Bcl2 chimeras are processed by the RNAi machinery resulting in the intended Ago2 cleavage product.

Finally, we investigated whether silencing of Bcl-2 by the aptamer-siRNA chimeras would sensitize N202.1A cells to cisplatin treatment (Figure 5F, Bcl2-chimeras). N202.1A cells were incubated with either the aptamer-siRNA chimeras alone (solid gray) or in combination with low dose cisplatin (20 μ M) (red line) for up to 96 h. High dose cisplatin (80 μ M) (blue line) was used as a positive control for apoptosis in these assays (Figure 5F, Bcl2-chimeras). Apoptosis was measured by flow cytometry using an antibody against active, cleaved caspase 3 as described earlier (Figure 4D). The average of three experiments was plotted (Supplementary Figure S5). Non-targeting chimeras (SCR1 and SCR2) were used to control for chimera induced-cell death in these assays. The percent of dead cells following treatment was also determined by the trypan blue stain assay (data not shown). Importantly, several of the chimeras tested

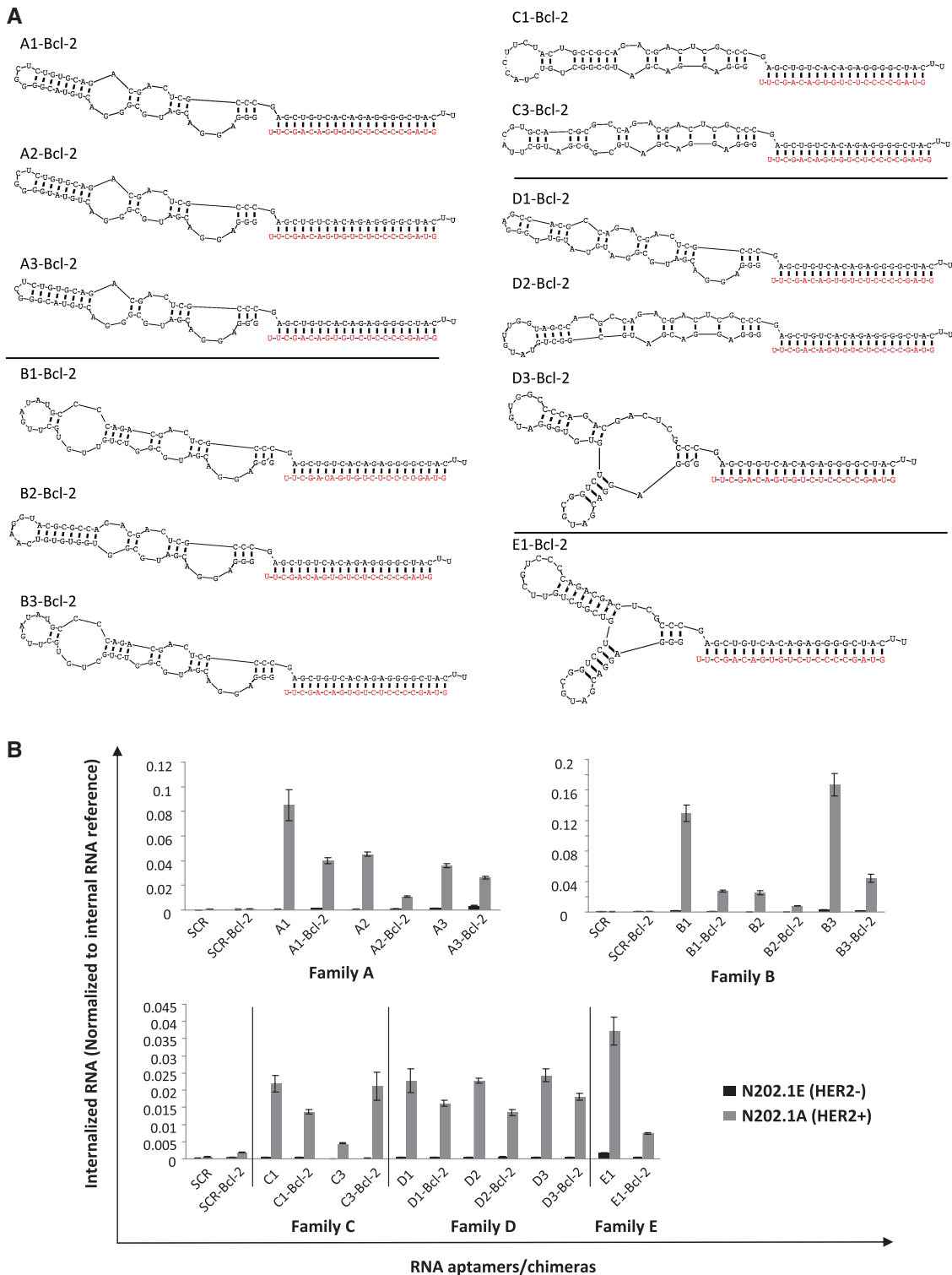


Figure 5. Chimera-mediated death of HER2⁺-mammary carcinoma cells. (A) Predicted secondary structures of the HER2 aptamers-Bcl-2 siRNA chimeras using RNAstructure. Red nucleotides indicate the Bcl-2 siRNA guide strand sequence. Chimeras were generated by annealing the Bcl-2 guide strand to the complementary passenger strand sequence covalently linked to the 3'-end of each aptamer. (B) Cell-type specific internalization of the aptamer-siRNA chimeras was compared to that of the aptamers alone and analyzed by qRT-PCR as in Figure 1C. (C) Internalization of chimeras in N202.1A(HER2⁺) cells versus normal mouse mammary carcinoma cells (NMuMG) (B). (D) Silencing of HER-2 at the mRNA level was determined by qRT-PCR after incubation of N202.1A(HER2⁺) cells with chimeras for 38 h (top panel) or 96 h (bottom panel). Bcl-2 mRNA levels were normalized to GAPDH mRNA levels for each sample. (E) 5'-Rapid amplification of cDNA ends (5'-RACE) PCR analysis to assess siRNA mediated cleavage of Bcl2 mRNA in cells treated with the various HER2-Bcl2 chimeras (A1-Bcl2, B1-Bcl2, C3-Bcl2, D1-Bcl2, E1-Bcl2). A non-internalizing chimera (SCR1-Bcl2) was used as a control in these assays. (F) N202.1A(HER2⁺) cells were treated with either aptamer-Bcl-2 siRNA chimeras (Bcl2-chimeras; top panels) or aptamer-control siRNA chimeras (Con-chimeras; bottom panels) for 72 h, then with media containing chimeras (solid gray) and low-dose cisplatin (20 μ M) (red line) for an additional 24 h. Following cisplatin treatment, cells were stained with an antibody to active cleaved caspase-3 and processed by flow cytometry to assess % apoptosis.

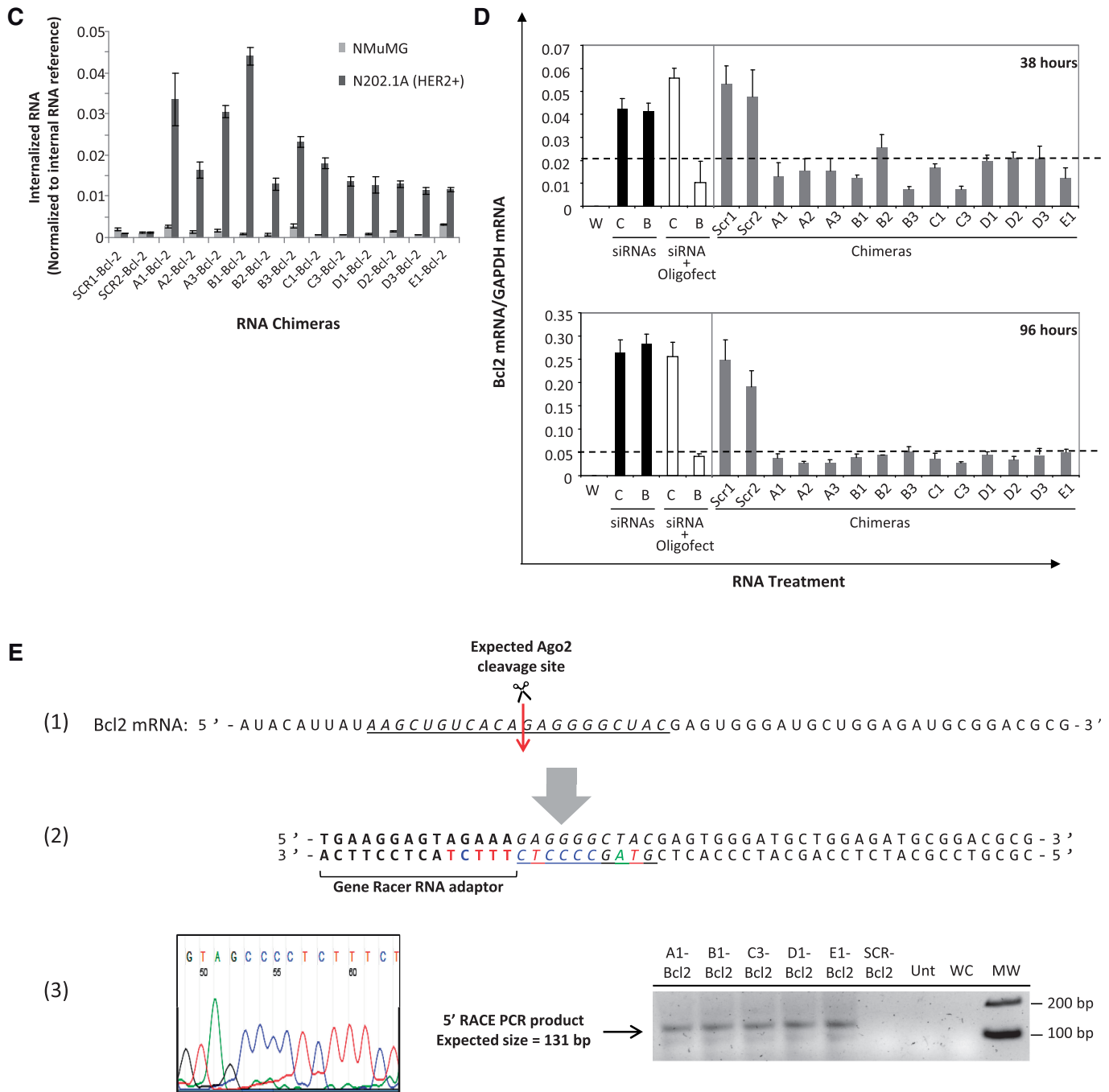


Figure 5. Continued.

(A1-Bcl2, A2-Bcl2, B3-Bcl-2, C1-Bcl2, C3-Bcl-2, D1-Bcl-2, D3-Bcl2 and E1-Bcl-2 chimeras), when combined with low dose cisplatin (20 μ M) (red line), resulted in a pronounced effect on cell death which was significantly greater than that obtained with either treatment alone and was comparable to that observed with high dose cisplatin (80 μ M). Interestingly, four (C3-Bcl2, D1-Bcl2, D3-Bcl2, E1-Bcl2) of the 12 chimeras tested, resulted in some level of apoptosis even in the absence of cisplatin treatment (see solid grey). This could be due to more

efficient processing of these chimeras by the RNAi machinery, rate of release of chimeras into the cytoplasm of target cells or potential modulation of HER2 pathways by the aptamer portion of the chimeras.

To investigate the role of the aptamer sequence on cell viability and cell sensitivity to low-dose cisplatin, for those HER2 chimeras that induce some degree of apoptosis in the absence of cisplatin (C3-Bcl2, D1-Bcl2, D3-Bcl2 and E1-Bcl2), we generated HER2 chimeras bearing a control, non-silencing siRNA sequence (Figure 5F, Con-chimeras).

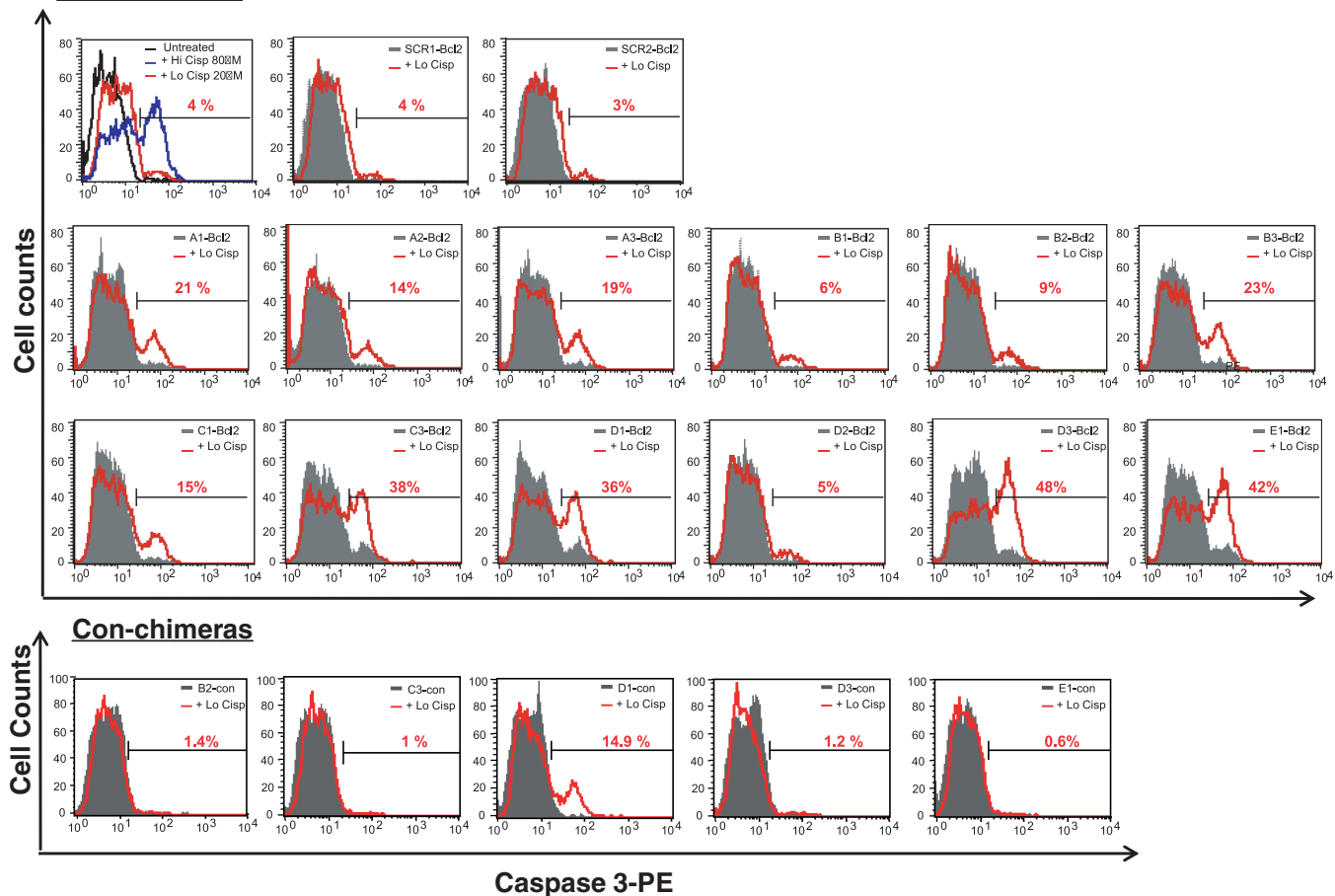
F Bcl2-chimeras

Figure 5. Continued.

In the absence of cisplatin, the control chimeras did not induce caspase 3 activation. When low-dose cisplatin was added to cells, no caspase activation was observed for control chimeras C3-con, D3-con or E1-con suggesting that the aptamer portion of these chimeras is not contributing to the cytotoxic effect observed. In contrast, and somewhat unexpectedly, in the presence of low-dose cisplatin D1-con chimera resulted in significant caspase 3 activation. This is likely due to the contribution of aptamer D1 sequence in modulating cellular pathways that confer chemosensitivity to cells. Together, these data suggest that the HER2-aptamer-Bcl-2 siRNA chimeras enhance the degree of chemosensitization in breast cancer cells.

To determine if the differences in the ability of the various chimeras to confer sensitivity to cells in the presence of low-dose cisplatin may be due to differential processing of the chimeras by the RNAi machinery, we performed a Small Fragment Northern (SFN) assay (Supplementary Figure S6; Supplementary Methods). This assay enables the quantification of processed mature siRNA inside a cell (90). In this experiment equal amounts of each of the chimeras were transfected into N202.1A cells using a cationic lipid to rule out potential differences between chimeras due to rate of uptake or release in the cytoplasm

of target cells. No significant differences in processing were observed for the various chimeras (see intensity of bands representing the antisense strands of processed RNAs) (Supplementary Figure S6). These data suggest that the HER2-Bcl2 chimeras are equally processed once inside the cell. Therefore, slight differences in silencing ability or ability to confer sensitivity to cells in the presence of low-dose cisplatin may be due to trafficking, potential modulation of HER2 pathways by the aptamer portion of the chimeras or non-specific immune stimulation by the chimeric RNAs.

To determine whether the effect on cells with regard to cell sensitivity to low dose cisplatin might be a result of non-specific immune activation, culture medium from cells treated with each of the chimeras was screened for levels of interferon- α (INT- α) and interleukin-6 (IL-6) using enzyme-linked immunosorbent assays (ELISA) (Supplementary Figure S7; Supplementary Methods). Importantly, no significant difference was seen in cytokine levels of mock treated cells (0 μ g/ml Poly I:C or PBS) or cells treated with the various HER2-Bcl2 chimeras. This was in contrast to cells treated with polyinosinic:polycytidylic acid (poly I:C), an established immune stimulator, suggesting that the chimeras are not triggering an innate immune response. Together, these

data confirm that the cell-sensitization effects are due to chimera mediated silencing and not to non-specific immune activation or differential processing of the chimeras by the RNAi machinery.

DISCUSSION

In this study, we demonstrate the utility of the 'cell-internalization SELEX' methodology for identifying target cell-specific RNA aptamers capable of delivering siRNAs into cells of interest. RNA aptamers that bind to rat HER2 with low nanomolar affinity and specificity (Figure 3) were isolated from a combinatorial SELEX library of 10^{12} RNA sequences by selecting for RNA sequences capable of binding to and internalizing into mouse mammary carcinoma cell lines expressing rat HER2 (Figure 2). The rat HER2 aptamers were covalently linked to siRNAs directed against the anti-apoptotic gene, Bcl-2 (Figure 5), whose expression is often elevated in breast cancers. When applied to mouse mammary carcinoma cell lines expressing rat HER2, the HER2 aptamer-Bcl2 siRNA chimeras internalized into the cells (Figure 5B and C) and silenced Bcl-2 gene expression (Figure 5D and E). Target specificity was demonstrated by showing that the chimeras do not internalize into matched control mouse mammary carcinoma cell lines that do not express rat HER2 (Figure 5B) or normal mouse mammary epithelial cells (NMuMG), which express negligible levels of mouse HER2 (Figure 5C). Importantly, Bcl-2 silencing in the HER2⁺-mouse mammary cancer cell lines resulted in increased sensitization of these cells to cisplatin treatment (Figure 5F), leading to apoptosis at significantly lower doses of the drug.

Delivery of siRNAs to specific cell-types *in vivo* has long been recognized as a significant obstacle to the clinical development of siRNA-based drugs. Targeted delivery has the dual advantage of reduced toxicity to normal surrounding tissues and of reduced effective therapeutic dose. Targeted approaches for siRNA delivery have included complex formulations with proteins/peptides (73,91–95), nanoparticles (73,96–99) or liposomes (100–103). Although, the preferred targeted delivery approach may be dependent on context, the aptamer-siRNA chimera approach has the advantage of simplicity (a single molecule rather than a complex mixture), safety (likely to be less immunogenic than proteins), ease of production (amenable to large scale chemical synthesis) and modifiability (amenable to chemical modifications for optimizing pharmacokinetics and pharmacodynamics) (74,104).

The work described herein is of importance in light of recent work by several groups, including ours, demonstrating the usefulness of RNA aptamers for delivering siRNAs and shRNAs to specific cell types *in vivo* (68,69,74,104–110). Initially, an RNA aptamer to a prostate cancer-specific surface antigen (PSMA) was successfully employed by us to target siRNAs directed against cancer-specific pro-survival genes into prostate cancer cells (68,74). Due to the simple design and ease

of production of the RNA aptamer-siRNA covalent assembly approach (68), several groups have since linked various silencing RNAs (siRNAs and shRNAs) to the A10 PSMA aptamer (and to truncated versions of A10) as a targeted therapy for prostate cancer (69,106). To date, efficient targeted delivery to prostate tumors has been demonstrated using siRNAs silencing cancer-specific pro-survival genes (to induce tumor death) (68,74) as well as genes involved in DNA repair (for sensitizing tumors to radiation) (69) and nonsense mRNA decay (NMD) (to mount an immune response to the tumor) pathways (106). In each case, the result of targeting the siRNAs was dramatic, leading to significant reduction in tumor burden in the treated mice. These studies demonstrate the flexibility of using one aptamer sequence for delivering siRNAs directed against many different therapeutic target genes, highlighting the potential of this technology for combinatorial gene targeting.

In addition to prostate cancer, aptamer-siRNA conjugates/chimeras have also been successfully generated as potential therapeutics (105,107,109,110) and prophylactics for HIV (108). The availability of cell-internalizing aptamers specific for the prostate cancer antigen, PSMA (111), the T-cell receptor, CD4 (108,112) and the HIV glycoprotein, gp120 (109,113), has made it possible to evaluate the use of RNA aptamers as delivery vehicles for siRNAs in these contexts and, more importantly, to establish design rules for optimal processing of the aptamer-siRNA conjugates by the RNAi machinery (74). However, a limiting factor for the broad applicability of this delivery technology is the relative paucity of candidate aptamers for specific delivery. Only a handful of aptamers that bind to cell surface receptors have been isolated due to difficulties in obtaining purified preparations of recombinant membrane proteins for selection. Cell-based selections for isolating aptamers with high affinity and specificity to cell surface proteins have been proposed as an alternative to selections performed *in vitro*. However, while these selections favor the identification of aptamers that bind to receptors in the cell membrane milieu, they do not necessarily enrich for aptamers that internalize into the target cells. The advantage of the 'cell-internalization SELEX' approach, described herein, is 2-fold: (i) it favors the isolation of RNAs that bind to receptors (e.g. HER2) in their native state and (ii) it enriches for RNAs that are internalized by the target cells.

Current aptamer-siRNA chimeras are, presumably, internalized by receptor-mediated internalization and released into the cytoplasm where they encounter the RNAi machinery. It has been argued that chimeras escape from endosomes prior to entering the lysosome where the presence of nucleases and low pH conditions are likely to result in siRNA degradation (114). However, currently, neither the uptake kinetics of aptamer-siRNA chimeras nor the molecular mechanisms by which these RNAs escape from the endosome are known. Thus, future optimization of this approach, to enable the identification of aptamers that internalize and that are released into the cytoplasm of target cells, awaits further elucidation of the molecular mechanisms of RNA aptamer uptake and trafficking.

In conclusion, we describe a novel approach that has enabled the identification of RNA aptamers capable of delivering chemo-sensitizing siRNAs to HER2-expressing cancer cells. While our proof-of-concept study made use of matched controlled cell lines derived from a rat HER2 transgenic mouse mammary carcinoma model, the work can be easily extended to identifying human specific aptamers. Furthermore, as discussed earlier, HER2 aptamers can be linked to different siRNAs directed against genes implicated in multiple cancer promoting pathways (e.g. growth, survival, metastasis). The combination of such HER2-targeting chimeras may maximize therapeutic efficacy and greatly reduce the likelihood of drug resistance in the context of malignant breast cancers.

SUPPLEMENTARY DATA

Supplementary Data is available at NAR Online: Supplementary Tables 1 and 2, Supplementary Figures 1–7 and Supplementary Methods.

ACKNOWLEDGEMENTS

We would like to thank Drs Eli Gilboa, Guido Forni, Ann Thor and Scott Oakes for providing critical cell lines and reagents and Drs Al Klingelutz and Eli Gilboa for critical review of the manuscript. Conceived and designed the experiments: K.W.T., L.I.H. and P.H.G. Performed the experiments: K.W.T., L.I.H., W.H.T., X.L., J.P.D., K.R.S., W.M.R., F.J.H. and P.H.G. Analyzed the data and interpreted experiments: K.W.T., L.I.H., W.H.T., W.M.R., F.J.H., J.O.M. and P.H.G. Wrote the paper: K.W.T., L.I.H. and P.H.G.

FUNDING

Funding for open access charge: National Institutes of Health [1RO1 CA138503-01 and 1R21DE019953-01 to P.H.G.]; Mary Kay Ash Charitable Foundation [001-09 to P.H.G.]; Ladies Auxiliary to the Veterans of Foreign Wars (VFW) Postdoctoral Fellowship [2008–2010, to K.W.T.] and T32 HL 07344-3 NIH T32 Institutional NRSA (2007) training grant (to K.W.T.).

Conflict of interest statement. None declared.

REFERENCES

- Jemal,A., Center,M.M., DeSantis,C. and Ward,E.M. (2010) Global patterns of cancer incidence and mortality rates and trends. *Cancer Epidemiol. Biomarkers Prev.*, **19**, 1893–1907.
- Jemal,A., Siegel,R., Xu,J. and Ward,E. (2010) Cancer statistics, 2010. *CA Cancer J. Clin.*, **60**, 277–300.
- Jemal,A., Ward,E. and Thun,M. (2010) Declining death rates reflect progress against cancer. *PLoS One*, **5**, e9584.
- DeSantis,C., Jemal,A., Ward,E. and Thun,M.J. (2008) Temporal trends in breast cancer mortality by state and race. *Cancer Causes Control*, **19**, 537–545.
- Moasser,M.M. (2007) Targeting the function of the HER2 oncogene in human cancer therapeutics. *Oncogene*, **26**, 6577–6592.
- Sundaresan,S., Penuel,E. and Sliwkowski,M.X. (1999) The biology of human epidermal growth factor receptor 2. *Curr. Oncol. Rep.*, **1**, 16–22.
- Yarden,Y. (2001) Biology of HER2 and its importance in breast cancer. *Oncology*, **61**(Suppl. 2), 1–13.
- Harari,D. and Yarden,Y. (2000) Molecular mechanisms underlying ErbB2/HER2 action in breast cancer. *Oncogene*, **19**, 6102–6114.
- Muthuswamy,S.K., Gilman,M. and Brugge,J.S. (1999) Controlled dimerization of ErbB receptors provides evidence for differential signaling by homo- and heterodimers. *Mol. Cell. Biol.*, **19**, 6845–6857.
- Karunagaran,D., Tzahar,E., Beerli,R.R., Chen,X., Graus-Porta,D., Ratzkin,B.J., Seger,R., Hynes,N.E. and Yarden,Y. (1996) ErbB-2 is a common auxiliary subunit of NDF and EGF receptors: implications for breast cancer. *EMBO J.*, **15**, 254–264.
- Davies,E. and Hiscox,S. (2011) New therapeutic approaches in breast cancer. *Maturitas*, **68**, 121–128.
- Higa,G.M., Singh,V. and Abraham,J. (2010) Biological considerations and clinical applications of new HER2-targeted agents. *Expert Rev. Anticancer Ther.*, **10**, 1497–1509.
- Slamon,D.J., Godolphin,W., Jones,L.A., Holt,J.A., Wong,S.G., Keith,D.E., Levin,W.J., Stuart,S.G., Udove,J. and Ullrich,A. (1989) Studies of the HER-2/neu proto-oncogene in human breast and ovarian cancer. *Science*, **244**, 707–712.
- Lemoine,N.R., Jain,S., Silvestre,F., Lopes,C., Hughes,C.M., McLelland,E., Gullick,W.J. and Filipe,M.I. (1991) Amplification and overexpression of the EGF receptor and c-erbB-2 proto-oncogenes in human stomach cancer. *Br. J. Cancer*, **64**, 79–83.
- De Vita,F., Giuliani,F., Silvestris,N., Catalano,G., Ciardiello,F. and Orditura,M. (2010) Human epidermal growth factor receptor 2 (HER2) in gastric cancer: a new therapeutic target. *Cancer Treat Rev.*, **36**(Suppl. 3), S11–S15.
- Sauter,G., Moch,H., Moore,D., Carroll,P., Kerschmann,R., Chew,K., Mihatsch,M.J., Gudat,F. and Waldman,F. (1993) Heterogeneity of erbB-2 gene amplification in bladder cancer. *Cancer Res.*, **53**, 2199–2203.
- Stenman,G., Sandros,J., Nordkvist,A., Mark,J. and Sahlin,P. (1991) Expression of the ERBB2 protein in benign and malignant salivary gland tumors. *Genes Chromosomes Cancer*, **3**, 128–135.
- Tateishi,M., Ishida,T., Mitsudomi,T., Kaneko,S. and Sugimachi,K. (1991) Prognostic value of c-erbB-2 protein expression in human lung adenocarcinoma and squamous cell carcinoma. *Eur. J. Cancer*, **27**, 1372–1375.
- Morris,S.R. and Carey,L.A. (2006) Trastuzumab and beyond: new possibilities for the treatment of HER2-positive breast cancer. *Oncology*, **20**, 1763–1771; discussion 1771–1772, 1774–1776.
- Valabrega,G., Montemurro,F. and Aglietta,M. (2007) Trastuzumab: mechanism of action, resistance and future perspectives in HER2-overexpressing breast cancer. *Ann. Oncol.*, **18**, 977–984.
- Baselga,J., Tripathy,D., Mendelsohn,J., Baughman,S., Benz,C.C., Dantis,L., Sklarin,N.T., Seidman,A.D., Hudis,C.A., Moore,J. et al. (1996) Phase II study of weekly intravenous recombinant humanized anti-p185HER2 monoclonal antibody in patients with HER2/neu-overexpressing metastatic breast cancer. *J. Clin. Oncol.*, **14**, 737–744.
- Cobleigh,M.A., Vogel,C.L., Tripathy,D., Robert,N.J., Scholl,S., Fehrenbacher,L., Wolter,J.M., Paton,V., Shak,S., Lieberman,G. et al. (1999) Multinational study of the efficacy and safety of humanized anti-HER2 monoclonal antibody in women who have HER2-overexpressing metastatic breast cancer that has progressed after chemotherapy for metastatic disease. *J. Clin. Oncol.*, **17**, 2639–2648.
- Vogel,C.L., Cobleigh,M.A., Tripathy,D., Gutheil,J.C., Harris,L.N., Fehrenbacher,L., Slamon,D.J., Murphy,M., Novotny,W.F., Burchmore,M. et al. (2002) Efficacy and safety of trastuzumab as a single agent in first-line treatment of HER2-overexpressing metastatic breast cancer. *J. Clin. Oncol.*, **20**, 719–726.
- Hubalek,M., Brunner,C., Matthä,K. and Marth,C. (2010) Resistance to HER2-targeted therapy: mechanisms of trastuzumab resistance and possible strategies to overcome unresponsiveness to treatment. *Wien. Med. Wochenschr.*, **160**, 506–512.

25. Montemurro, F., Donadio, M., Clavarezza, M., Redana, S., Jacomuzzi, M.E., Valabrega, G., Danese, S., Vietti-Ramus, G., Durando, A., Venturini, M. *et al.* (2006) Outcome of patients with HER2-positive advanced breast cancer progressing during trastuzumab-based therapy. *Oncologist*, **11**, 318–324.
26. Montemurro, F., Valabrega, G. and Aglietta, M. (2006) Trastuzumab treatment in breast cancer. *N. Engl. J. Med.*, **354**, 2186; author reply 2186.
27. Marty, M., Cognetti, F., Maraninchi, D., Snyder, R., Mauriac, L., Tubiana-Hulin, M., Chan, S., Grimes, D., Anton, A., Lluch, A. *et al.* (2005) Randomized phase II trial of the efficacy and safety of trastuzumab combined with docetaxel in patients with human epidermal growth factor receptor 2-positive metastatic breast cancer administered as first-line treatment: the M77001 study group. *J. Clin. Oncol.*, **23**, 4265–4274.
28. Nahta, R. and Esteva, F.J. (2006) HER2 therapy: molecular mechanisms of trastuzumab resistance. *Breast Cancer Res.*, **8**, 215.
29. Nahta, R. and Esteva, F.J. (2006) Herceptin: mechanisms of action and resistance. *Cancer Lett.*, **232**, 123–138.
30. Nahta, R., Yu, D., Hung, M.C., Hortobagyi, G.N. and Esteva, F.J. (2006) Mechanisms of disease: understanding resistance to HER2-targeted therapy in human breast cancer. *Nat. Clin. Pract. Oncol.*, **3**, 269–280.
31. Camirand, A., Lu, Y. and Pollak, M. (2002) Co-targeting HER2/ ErbB2 and insulin-like growth factor-1 receptors causes synergistic inhibition of growth in HER2-overexpressing breast cancer cells. *Med. Sci. Monit.*, **8**, BR521–BR526.
32. Nahta, R., Yuan, L.X., Zhang, B., Kobayashi, R. and Esteva, F.J. (2005) Insulin-like growth factor-I receptor/human epidermal growth factor receptor 2 heterodimerization contributes to trastuzumab resistance of breast cancer cells. *Cancer Res.*, **65**, 11118–11128.
33. Chakraborty, A.K., Liang, K. and DiGiovanna, M.P. (2008) Co-targeting insulin-like growth factor I receptor and HER2: dramatic effects of HER2 inhibitors on nonoverexpressing breast cancer. *Cancer Res.*, **68**, 1538–1545.
34. Ritter, C.A., Perez-Torres, M., Rinehart, C., Guix, M., Dugger, T., Engelman, J.A. and Arteaga, C.L. (2007) Human breast cancer cells selected for resistance to trastuzumab in vivo overexpress epidermal growth factor receptor and ErbB ligands and remain dependent on the ErbB receptor network. *Clin. Cancer Res.*, **13**, 4909–4919.
35. Wheeler, D.L., Huang, S., Kruser, T.J., Nechrebecki, M.M., Armstrong, E.A., Benavente, S., Gondi, V., Hsu, K.T. and Harari, P.M. (2008) Mechanisms of acquired resistance to cetuximab: role of HER (ErbB) family members. *Oncogene*, **27**, 3944–3956.
36. Sergina, N.V., Rausch, M., Wang, D., Blair, J., Hann, B., Shokat, K.M. and Moasser, M.M. (2007) Escape from HER-family tyrosine kinase inhibitor therapy by the kinase-inactive HER3. *Nature*, **445**, 437–441.
37. Wang, S., Huang, X., Lee, C.K. and Liu, B. (2010) Elevated expression of erbB3 confers paclitaxel resistance in erbB2-overexpressing breast cancer cells via upregulation of Survivin. *Oncogene*, **29**, 4225–4236.
38. Brantley-Sieders, D.M., Zhuang, G., Hicks, D., Fang, W.B., Hwang, Y., Cates, J.M., Coffman, K., Jackson, D., Bruckheimer, E., Muraoka-Cook, R.S. *et al.* (2008) The receptor tyrosine kinase EphA2 promotes mammary adenocarcinoma tumorigenesis and metastatic progression in mice by amplifying ErbB2 signaling. *J. Clin. Invest.*, **118**, 64–78.
39. Kwong, K.Y. and Hung, M.C. (1998) A novel splice variant of HER2 with increased transformation activity. *Mol. Carcinog.*, **23**, 62–68.
40. Siegel, P.M., Ryan, E.D., Cardiff, R.D. and Muller, W.J. (1999) Elevated expression of activated forms of Neu/ErbB-2 and ErbB-3 are involved in the induction of mammary tumors in transgenic mice: implications for human breast cancer. *EMBO J.*, **18**, 2149–2164.
41. Castiglioni, F., Tagliabue, E., Campiglio, M., Pupa, S.M., Balsari, A. and Menard, S. (2006) Role of exon-16-deleted HER2 in breast carcinomas. *Endocr. Relat. Cancer*, **13**, 221–232.
42. Cittelly, D.M., Das, P.M., Salvo, V.A., Fonseca, J.P., Burow, M.E. and Jones, F.E. (2010) Oncogenic HER2{Delta}16 suppresses miR-15a/16 and deregulates BCL-2 to promote endocrine resistance of breast tumors. *Carcinogenesis*, **31**, 2049–2057.
43. Mitra, D., Brumlik, M.J., Okamgba, S.U., Zhu, Y., Duplessis, T.T., Parvani, J.G., Lesko, S.M., Brogi, E. and Jones, F.E. (2009) An oncogenic isoform of HER2 associated with locally disseminated breast cancer and trastuzumab resistance. *Mol. Cancer Ther.*, **8**, 2152–2162.
44. Reed, J.C. (2006) Proapoptotic multidomain Bcl-2/Bax-family proteins: mechanisms, physiological roles, and therapeutic opportunities. *Cell Death Differ.*, **13**, 1378–1386.
45. Kallel-Bayouh, I., Hassen, H.B., Khabir, A., Boujelbene, N., Daoud, J., Frikha, M., Sallemi-Boudawara, T., Aifa, S. and Rebai, A. (2010) Bcl-2 expression and triple negative profile in breast carcinoma. *Med. Oncol.*, **28**(Suppl. 1), s55–s61.
46. Ogretmen, B. and Safa, A.R. (1996) Down-regulation of apoptosis-related bcl-2 but not bcl-xL or bax proteins in multidrug-resistant MCF-7/Adr human breast cancer cells. *Int. J. Cancer*, **67**, 608–614.
47. Teixeira, C., Reed, J.C. and Pratt, M.A. (1995) Estrogen promotes chemotherapeutic drug resistance by a mechanism involving Bcl-2 proto-oncogene expression in human breast cancer cells. *Cancer Res.*, **55**, 3902–3907.
48. Real, P.J., Cao, Y., Wang, R., Nikolovska-Coleska, Z., Sanz-Ortiz, J., Wang, S. and Fernandez-Luna, J.L. (2004) Breast cancer cells can evade apoptosis-mediated selective killing by a novel small molecule inhibitor of Bcl-2. *Cancer Res.*, **64**, 7947–7953.
49. Huang, Y., Ray, S., Reed, J.C., Ibrado, A.M., Tang, C., Nawabi, A. and Bhalla, K. (1997) Estrogen increases intracellular p26Bcl-2 to p21Bax ratios and inhibits taxol-induced apoptosis of human breast cancer MCF-7 cells. *Breast Cancer Res. Treat.*, **42**, 73–81.
50. Kumar, R., Mandal, M., Lipton, A., Harvey, H. and Thompson, C.B. (1996) Overexpression of HER2 modulates bcl-2, bcl-XL, and tamoxifen-induced apoptosis in human MCF-7 breast cancer cells. *Clin. Cancer Res.*, **2**, 1215–1219.
51. Asanuma, H., Torigoe, T., Kamiguchi, K., Hirohashi, Y., Ohmura, T., Hirata, K., Sato, M. and Sato, N. (2005) Survivin expression is regulated by coexpression of human epidermal growth factor receptor 2 and epidermal growth factor receptor via phosphatidylinositol 3-kinase/AKT signaling pathway in breast cancer cells. *Cancer Res.*, **65**, 11018–11025.
52. Hinnis, A.R., Luckett, J.C. and Walker, R.A. (2007) Survivin is an independent predictor of short-term survival in poor prognostic breast cancer patients. *Br. J. Cancer*, **96**, 639–645.
53. Xia, W., Bisi, J., Strum, J., Liu, L., Carrick, K., Graham, K.M., Treece, A.L., Hardwicke, M.A., Dush, M., Liao, Q. *et al.* (2006) Regulation of survivin by ErbB2 signaling: therapeutic implications for ErbB2-overexpressing breast cancers. *Cancer Res.*, **66**, 1640–1647.
54. Ryan, B.M., Konecny, G.E., Kahlert, S., Wang, H.J., Untch, M., Meng, G., Pegram, M.D., Podratz, K.C., Crown, J., Slamon, D.J. *et al.* (2006) Survivin expression in breast cancer predicts clinical outcome and is associated with HER2, VEGF, urokinase plasminogen activator and PAI-1. *Ann. Oncol.*, **17**, 597–604.
55. Singh, M., Bleile, M.J., Shroyer, A.L., Heinz, D., Jarboe, E.A. and Shroyer, K.R. (2004) Analysis of survivin expression in a spectrum of benign to malignant lesions of the breast. *Appl. Immunohistochem. Mol. Morphol.*, **12**, 296–304.
56. Foster, F.M., Owens, T.W., Tanianis-Hughes, J., Clarke, R.B., Brennan, K., Bundred, N.J. and Streuli, C.H. (2009) Targeting inhibitor of apoptosis proteins in combination with ErbB antagonists in breast cancer. *Breast Cancer Res.*, **11**, R41.
57. Jha, K., Shukla, M. and Pandey, M. (2012) Survivin expression and targeting in breast cancer. *Surg. Oncol.*, **21**, 125–131.
58. Lima, R.T., Martins, L.M., Guimarães, J.E., Sambade, C. and Vasconcelos, M.H. (2004) Specific downregulation of bcl-2 and xIAP by RNAi enhances the effects of chemotherapeutic agents in MCF-7 human breast cancer cells. *Cancer Gene Ther.*, **11**, 309–316.
59. Akar, U., Chaves-Reyez, A., Barria, M., Tari, A., Sanguino, A., Kondo, Y., Kondo, S., Arun, B., Lopez-Berestein, G. and Ozpolat, B. (2008) Silencing of Bcl-2 expression by small interfering RNA induces autophagic cell death in MCF-7 breast cancer cells. *Autophagy*, **4**, 669–679.

60. Siddiqua, A., Long, L.M., Li, L., Marciniak, R.A. and Kazhdan, I. (2008) Expression of HER-2 in MCF-7 breast cancer cells modulates anti-apoptotic proteins Survivin and Bcl-2 via the extracellular signal-related kinase (ERK) and phosphoinositide-3 kinase (PI3K) signalling pathways. *BMC Cancer*, **8**, 129.
61. Fire, A., Xu, S., Montgomery, M.K., Kostas, S.A., Driver, S.E. and Mello, C.C. (1998) Potent and specific genetic interference by double-stranded RNA in *Caenorhabditis elegans*. *Nature*, **391**, 806–811.
62. Bumcrot, D., Manoharan, M., Koteliensky, V. and Sah, D.W. (2006) RNAi therapeutics: a potential new class of pharmaceutical drugs. *Nat. Chem. Biol.*, **2**, 711–719.
63. Soutschek, J., Akinc, A., Bramlage, B., Charisse, K., Constien, R., Donoghue, M., Elbashir, S., Geick, A., Hadwiger, P., Harborth, J. et al. (2004) Therapeutic silencing of an endogenous gene by systemic administration of modified siRNAs. *Nature*, **432**, 173–178.
64. Pai, S.I., Lin, Y.Y., Macaes, B., Meneshian, A., Hung, C.F. and Wu, T.C. (2006) Prospects of RNA interference therapy for cancer. *Gene Ther.*, **13**, 464–477.
65. Petrocca, F. and Lieberman, J. (2011) Promise and challenge of RNA interference-based therapy for cancer. *J. Clin. Oncol.*, **29**, 747–754.
66. Sioud, M. (2011) Promises and challenges in developing RNAi as a research tool and therapy. *Methods Mol. Biol.*, **703**, 173–187.
67. Hao, J.H., Gu, Q.L., Liu, B.Y., Li, J.F., Chen, X.H., Ji, Y.B., Zhu, Z.G. and Lin, Y.Z. (2007) Inhibition of the proliferation of human gastric cancer cells SGC-7901 in vitro and in vivo using Bcl-2 siRNA. *Chin. Med. J.*, **120**, 2105–2111.
68. McNamara, J.O. II, Andrechek, E.R., Wang, Y., Viles, K.D., Rempel, R.E., Gilboa, E., Sullenger, B.A. and Giangrande, P.H. (2006) Cell type-specific delivery of siRNAs with aptamer-siRNA chimeras. *Nat. Biotechnol.*, **24**, 1005–1015.
69. Ni, X., Zhang, Y., Ribas, J., Chowdhury, W.H., Castanares, M., Zhang, Z., Laiho, M., DeWeese, T.L. and Lupold, S.E. (2011) Prostate-targeted radiosensitization via aptamer-shRNA chimeras in human tumor xenografts. *J. Clin. Invest.*, **121**, 2383–2390.
70. Pecot, C.V., Calin, G.A., Coleman, R.L., Lopez-Berestein, G. and Sood, A.K. (2011) RNA interference in the clinic: challenges and future directions. *Nat. Rev. Cancer*, **11**, 59–67.
71. Lares, M.R., Rossi, J.J. and Ouellet, D.L. (2010) RNAi and small interfering RNAs in human disease therapeutic applications. *Trends Biotechnol.*, **28**, 570–579.
72. Manjunath, N. and Dykxhoorn, D.M. (2010) Advances in synthetic siRNA delivery. *Discov. Med.*, **9**, 418–430.
73. Higuchi, Y., Kawakami, S. and Hashida, M. (2010) Strategies for in vivo delivery of siRNAs: recent progress. *BioDrugs*, **24**, 195–205.
74. Dassie, J.P., Liu, X.Y., Thomas, G.S., Whitaker, R.M., Thiel, K.W., Stockdale, K.R., Meyerholz, D.K., McCaffrey, A.P., McNamara, J.O. II and Giangrande, P.H. (2009) Systemic administration of optimized aptamer-siRNA chimeras promotes regression of PSMA-expressing tumors. *Nat. Biotechnol.*, **27**, 839–849.
75. Lollini, P.L., Nicoletti, G., Landuzzi, L., De Giovanni, C., Rossi, I., Di Carlo, E., Musiani, P., Muller, W.J. and Nanni, P. (1998) Down regulation of major histocompatibility complex class I expression in mammary carcinoma of HER-2/neu transgenic mice. *Int. J. Cancer*, **77**, 937–941.
76. Nanni, P., Pupa, S.M., Nicoletti, G., De Giovanni, C., Landuzzi, L., Rossi, I., Astolfi, A., Ricci, C., De Vecchi, R., Invernizzi, A.M. et al. (2000) p185(neu) protein is required for tumor and anchorage-independent growth, not for cell proliferation of transgenic mammary carcinoma. *Int. J. Cancer*, **87**, 186–194.
77. Kim, A., Liu, B., Ordonez-Ercan, D., Alvarez, K.M., Jones, L.D., McKimney, C., Edgerton, S.M., Yang, X. and Thor, A.D. (2005) Functional interaction between mouse erbB3 and wild-type rat c-neu in transgenic mouse mammary tumor cells. *Breast Cancer Res.*, **7**, R708–R718.
78. Liu, F.F., Stone, J.R., Schuldt, A.J., Okoshi, K., Okoshi, M.P., Nakayama, M., Ho, K.K., Manning, W.J., Marchionni, M.A., Lorell, B.H. et al. (2005) Heterozygous knockout of neurotrophin-1 gene in mice exacerbates doxorubicin-induced heart failure. *Am. J. Physiol. Heart Circ. Physiol.*, **289**, H660–H666.
79. Oakes, S.A., Scorrano, L., Opferman, J.T., Bassik, M.C., Nishino, M., Pozzan, T. and Korsmeyer, S.J. (2005) Proapoptotic BAX and BAK regulate the type 1 inositol triphosphate receptor and calcium leak from the endoplasmic reticulum. *Proc. Natl Acad. Sci. USA*, **102**, 105–110.
80. Cerchia, L., Ducongé, F., Pestourie, C., Boulay, J., Aissouni, Y., Gombert, K., Tavitian, B., de Franciscis, V. and Libri, D. (2005) Neutralizing aptamers from whole-cell SELEX inhibit the RET receptor tyrosine kinase. *PLoS Biol.*, **3**, e123.
81. Padilla, R. and Sousa, R. (1999) Efficient synthesis of nucleic acids heavily modified with non-canonical ribose 2'-groups using a mutant T7 RNA polymerase (RNAP). *Nucleic Acids Res.*, **27**, 1561–1563.
82. Larkin, M.A., Blackshields, G., Brown, N.P., Chenna, R., McGettigan, P.A., McWilliam, H., Valentin, F., Wallace, I.M., Wilm, A., Lopez, R. et al. (2007) Clustal W and Clustal X version 2.0. *Bioinformatics*, **23**, 2947–2948.
83. McNamara, J.O., Kolonias, D., Pastor, F., Mittler, R.S., Chen, L., Giangrande, P.H., Sullenger, B. and Gilboa, E. (2008) Multivalent 4-1BB binding aptamers costimulate CD8+ T cells and inhibit tumor growth in mice. *J. Clin. Invest.*, **118**, 376–386.
84. Hernandez, F.J., Dondapati, S.K., Ozalp, V.C., Pinto, A., O'Sullivan, C.K., Klar, T.A. and Katakis, I. (2009) Label free optical sensor for Avidin based on single gold nanoparticles functionalized with aptamers. *J. Biophotonics*, **2**, 227–231.
85. Hernandez, F.J., Kalra, N., Wengel, J. and Vester, B. (2009) Aptamers as a model for functional evaluation of LNA and 2'-amino LNA. *Bioorg. Med. Chem. Lett.*, **19**, 6585–6587.
86. Thiel, W.H., Bair, T., Wyatt Thiel, K., Dassie, J.P., Rockey, W.M., Howell, C.A., Liu, X.Y., Dupuy, A.J., Huang, L., Owczarzy, R. et al. (2011) Nucleotide bias observed with a short SELEX RNA aptamer library. *Nucleic Acid Ther.*, **21**, 253–263.
87. Reed, J.C. (1995) Bcl-2: prevention of apoptosis as a mechanism of drug resistance. *Hematol. Clin. North Am.*, **9**, 451–473.
88. Huang, Y., Ibrado, A.M., Reed, J.C., Bullock, G., Ray, S., Tang, C. and Bhalla, K. (1997) Co-expression of several molecular mechanisms of multidrug resistance and their significance for paclitaxel cytotoxicity in human AML HL-60 cells. *Leukemia*, **11**, 253–257.
89. Reed, J.C., Miyashita, T., Takayama, S., Wang, H.G., Sato, T., Krajewski, S., Aimé-Sempé, C., Bodrug, S., Kitada, S. and Hanada, M. (1996) BCL-2 family proteins: regulators of cell death involved in the pathogenesis of cancer and resistance to therapy. *J. Cell. Biochem.*, **60**, 23–32.
90. Pall, G.S. and Hamilton, A.J. (2008) Improved northern blot method for enhanced detection of small RNA. *Nat. Protoc.*, **3**, 1077–1084.
91. Song, E., Zhu, P., Lee, S.K., Chowdhury, D., Kussman, S., Dykxhoorn, D.M., Feng, Y., Palliser, D., Weiner, D.B., Shankar, P. et al. (2005) Antibody mediated in vivo delivery of small interfering RNAs via cell-surface receptors. *Nat. Biotechnol.*, **23**, 709–717.
92. Vornlocher, H.P. (2006) Antibody-directed cell-type-specific delivery of siRNA. *Trends Mol. Med.*, **12**, 1–3.
93. Meade, B.R. and Dowdy, S.F. (2007) Exogenous siRNA delivery using peptide transduction domains/cell penetrating peptides. *Adv. Drug Deliv. Rev.*, **59**, 134–140.
94. Ikeda, Y. and Taira, K. (2006) Ligand-targeted delivery of therapeutic siRNA. *Pharm. Res.*, **23**, 1631–1640.
95. Eguchi, A. and Dowdy, S.F. (2009) siRNA delivery using peptide transduction domains. *Trends Pharmacol. Sci.*, **30**, 341–345.
96. Song, W.J., Du, J.Z., Sun, T.M., Zhang, P.Z. and Wang, J. (2010) Gold nanoparticles capped with polyethyleneimine for enhanced siRNA delivery. *Small*, **6**, 239–246.
97. Toub, N., Malvy, C., Fattal, E. and Couvreur, P. (2006) Innovative nanotechnologies for the delivery of oligonucleotides and siRNA. *Biomed. Pharmacother.*, **60**, 607–620.
98. Tamura, A. and Nagasaki, Y. (2010) Smart siRNA delivery systems based on polymeric nanoassemblies and nanoparticles. *Nanomedicine*, **5**, 1089–1102.
99. Gao, W., Xiao, Z., Radovic-Moreno, A., Shi, J., Langer, R. and Farokhzad, O.C. (2010) Progress in siRNA delivery using multifunctional nanoparticles. *Methods Mol. Biol.*, **629**, 53–67.

100. Sioud, M. and Sorensen, D.R. (2003) Cationic liposome-mediated delivery of siRNAs in adult mice. *Biochem. Biophys. Res. Commun.*, **312**, 1220–1225.
101. Pal, A., Ahmad, A., Khan, S., Sakabe, I., Zhang, C., Kasid, U.N. and Ahmad, I. (2005) Systemic delivery of RafsiRNA using cationic cardiolipin liposomes silences Raf-1 expression and inhibits tumor growth in xenograft model of human prostate cancer. *Int. J. Oncol.*, **26**, 1087–1091.
102. Morrissey, D.V., Lockridge, J.A., Shaw, L., Blanchard, K., Jensen, K., Breen, W., Hartsough, K., Machemer, L., Radka, S., Jadhav, V. *et al.* (2005) Potent and persistent in vivo anti-HBV activity of chemically modified siRNAs. *Nat. Biotechnol.*, **23**, 1002–1007.
103. Wu, S.Y. and McMillan, N.A. (2009) Lipidic systems for in vivo siRNA delivery. *AAPS J.*, **11**, 639–652.
104. Thiel, K.W. and Giangrande, P.H. (2010) Intracellular delivery of RNA-based therapeutics using aptamers. *Ther. Deliv.*, **1**, 849–861.
105. Neff, C.P., Zhou, J., Remling, L., Kuruvilla, J., Zhang, J., Li, H., Smith, D.D., Swiderski, P., Rossi, J.J. and Akkina, R. (2011) An aptamer-siRNA chimera suppresses HIV-1 viral loads and protects from helper CD4(+) T cell decline in humanized mice. *Sci. Transl. Med.*, **3**, 66ra6.
106. Pastor, F., Kolonias, D., Giangrande, P.H. and Gilboa, E. (2010) Induction of tumour immunity by targeted inhibition of nonsense-mediated mRNA decay. *Nature*, **465**, 227–230.
107. Zhou, J. and Rossi, J.J. (2010) Aptamer-targeted cell-specific RNA interference. *Silence*, **1**, 4.
108. Wheeler, L.A., Trifonova, R., Vrbanc, V., Basar, E., McKernan, S., Xu, Z., Seung, E., Deruaz, M., Dudek, T., Einarsson, J.I. *et al.* (2011) Inhibition of HIV transmission in human cervicovaginal explants and humanized mice using CD4 aptamer-siRNA chimeras. *J. Clin. Invest.*, **121**, 2401–2412.
109. Zhou, J., Swiderski, P., Li, H., Zhang, J., Neff, C.P., Akkina, R. and Rossi, J.J. (2009) Selection, characterization and application of new RNA HIV gp 120 aptamers for facile delivery of Dicer substrate siRNAs into HIV infected cells. *Nucleic Acids Res.*, **37**, 3094–3109.
110. Zhou, J., Li, H., Li, S., Zaia, J. and Rossi, J.J. (2008) Novel dual inhibitory function aptamer-siRNA delivery system for HIV-1 therapy. *Mol. Ther.*, **16**, 1481–1489.
111. Lupold, S.E., Hicke, B.J., Lin, Y. and Coffey, D.S. (2002) Identification and characterization of nuclease-stabilized RNA molecules that bind human prostate cancer cells via the prostate-specific membrane antigen. *Cancer Res.*, **62**, 4029–4033.
112. Kraus, E., James, W. and Barclay, A.N. (1998) Cutting edge: novel RNA ligands able to bind CD4 antigen and inhibit CD4+ T lymphocyte function. *J. Immunol.*, **160**, 5209–5212.
113. Zhou, J., Shu, Y., Guo, P., Smith, D.D. and Rossi, J.J. (2011) Dual functional RNA nanoparticles containing phi29 motor pRNA and anti-gp120 aptamer for cell-type specific delivery and HIV-1 Inhibition. *Methods*, 284–294.
114. Dominska, M. and Dykxhoorn, D.M. (2010) Breaking down the barriers: siRNA delivery and endosome escape. *J. Cell Sci.*, **123**, 1183–1189.